

MARTIN MARIETTA ENERGY SYSTEMS LIBRARIES



3 4456 0365943 1

ORNL-3469  
UC-34 - Physics  
TID-4500 (23rd ed.)

MEASUREMENT OF SPECTRAL DISTRIBUTION OF  
POSITRON FLUX IN AN INFINITE COPPER  
MEDIUM CONTAINING  $\text{Cu}^{64}$

W. H. Wilkie  
R. D. Birkhoff  
(Thesis)

CENTRAL RESEARCH LIBRARY  
DOCUMENT COLLECTION

**LIBRARY LOAN COPY**

**DO NOT TRANSFER TO ANOTHER PERSON**

If you wish someone else to see this  
document, send in name with document  
and the library will arrange a loan.



**OAK RIDGE NATIONAL LABORATORY**

operated by

**UNION CARBIDE CORPORATION**

for the

**U.S. ATOMIC ENERGY COMMISSION**

LEGAL NOTICE

This report was prepared as an account of Government sponsored work. Neither the United States, nor the Commission, nor any person acting on behalf of the Commission:

- A. Makes any warranty or representation, expressed or implied, with respect to the accuracy, completeness, or usefulness of the information contained in this report, or that the use of any information, apparatus, method, or process disclosed in this report may not infringe privately owned rights; or
- B. Assumes any liabilities with respect to the use of, or for damages resulting from the use of any information, apparatus, method, or process disclosed in this report.

As used in the above, "person acting on behalf of the Commission" includes any employee or contractor of the Commission, or employee of such contractor, to the extent that such employee or contractor of the Commission, or employee of such contractor prepares, disseminates, or provides access to, any information pursuant to his employment or contract with the Commission, or his employment with such contractor.

ORNL 3469

Contract No. W-7405-eng-26

Health Physics Division

MEASUREMENT OF SPECTRAL DISTRIBUTION OF POSITRON FLUX IN AN  
INFINITE COPPER MEDIUM CONTAINING Cu<sup>64</sup>

W. H. Wilkie  
R. D. Birkhoff

(Submitted as a thesis to the Faculty of the Graduate School of  
Vanderbilt University in partial fulfillment of the requirements  
for the degree of Master of Science in Physics)

DATE ISSUED

DEC 10 1963

OAK RIDGE NATIONAL LABORATORY  
Oak Ridge, Tennessee  
operated by  
UNION CARBIDE CORPORATION  
for the  
U. S. ATOMIC ENERGY COMMISSION



3 4456 0365943 1



## ACKNOWLEDGMENTS

Appreciation is extended to H. H. Hubbell, Jr. (ORNL) for his many valuable comments and suggestions with all phases of the research. I wish to thank J. A. Harter (ORNL) for his helpful advice and assistance with the electronic problems.

I would also like to extend my appreciation to P. W. Reinhardt (ORNL) and F. J. Davis (ORNL) for their helpful suggestions and their kind cooperation with the use of their equipment. Grateful recognition is given to P. N. Hensley (ORNL) and G. H. Hager (ORNL) for their help with the engineering aspects of the research.

Further appreciation is extended to the Oak Ridge Institute of Nuclear Studies which made this research possible through the AEC Special Fellowship in Health Physics.

## ABSTRACT

The spectral distribution of the flux of positrons inside a beta radioactive medium has been experimentally determined using an anthracene coincidence scintillation spectrometer. Positrons leaving a copper cavity source containing  $\text{Cu}^{64}$  were absorbed in a thin anthracene crystal. The light pulse from the anthracene was recorded in a 256 channel analyzer if a NaI scintillation spectrometer nearby recorded simultaneously a count under the total absorption peak for annihilation radiation. Thus discrimination against negative and secondary electrons was obtained which permitted observation of the primary positron slowing down flux. Data were corrected for the non-linear pulse height vs. energy relationship in anthracene by a semi-empirical theory due to Birks, the validity of which was demonstrated by its use in obtaining a linear Fermi plot of  $\text{Pm}^{147}$ . Positron spectra were corrected also for Compton absorption of the annihilation radiation in the anthracene.

Results were compared with the theoretical continuous-slowing-down model. Over the energy range measured (20-650 keV) it was concluded that the continuous-slowing-down model gives the correct shape for the primary slowing-down spectrum.

## TABLE OF CONTENTS

	page
ACKNOWLEDGMENTS -----	iii
LIST OF TABLES -----	vii
LIST OF FIGURES -----	viii
CHAPTER	
I. INTRODUCTION -----	1
II. THEORY -----	3
A. Beta Spectra -----	3
1. Continuous-Slowing-Down Theory -----	3
2. Effect of Coincident Pulses in Positron Spectra -----	11
B. Nonlinearities Inherent in the Scintillation Method -----	15
1. Crystal Nonlinearity -----	15
2. Bandwidth Correction -----	27
III. ELECTRONIC APPARATUS -----	30
IV. ANTHRACENE SPECTROMETER -----	34
A. Construction -----	34
B. Source Preparation -----	37
1. Barium-137 -----	37
2. Promethium-147 -----	38
3. Copper-64 -----	39
C. Calibration -----	42
1. Barium-137 -----	42
2. Mercury Relay Pulse Generator -----	46
3. Promethium-147 -----	49

TABLE OF CONTENTS (Con't)

	page
V. COPPER-64 SPECTRA -----	52
VI. DISCUSSION -----	60
APPENDIX	
Determination of the Average Activity During a Time Interval -----	61
BIBLIOGRAPHY -----	62

LIST OF TABLES

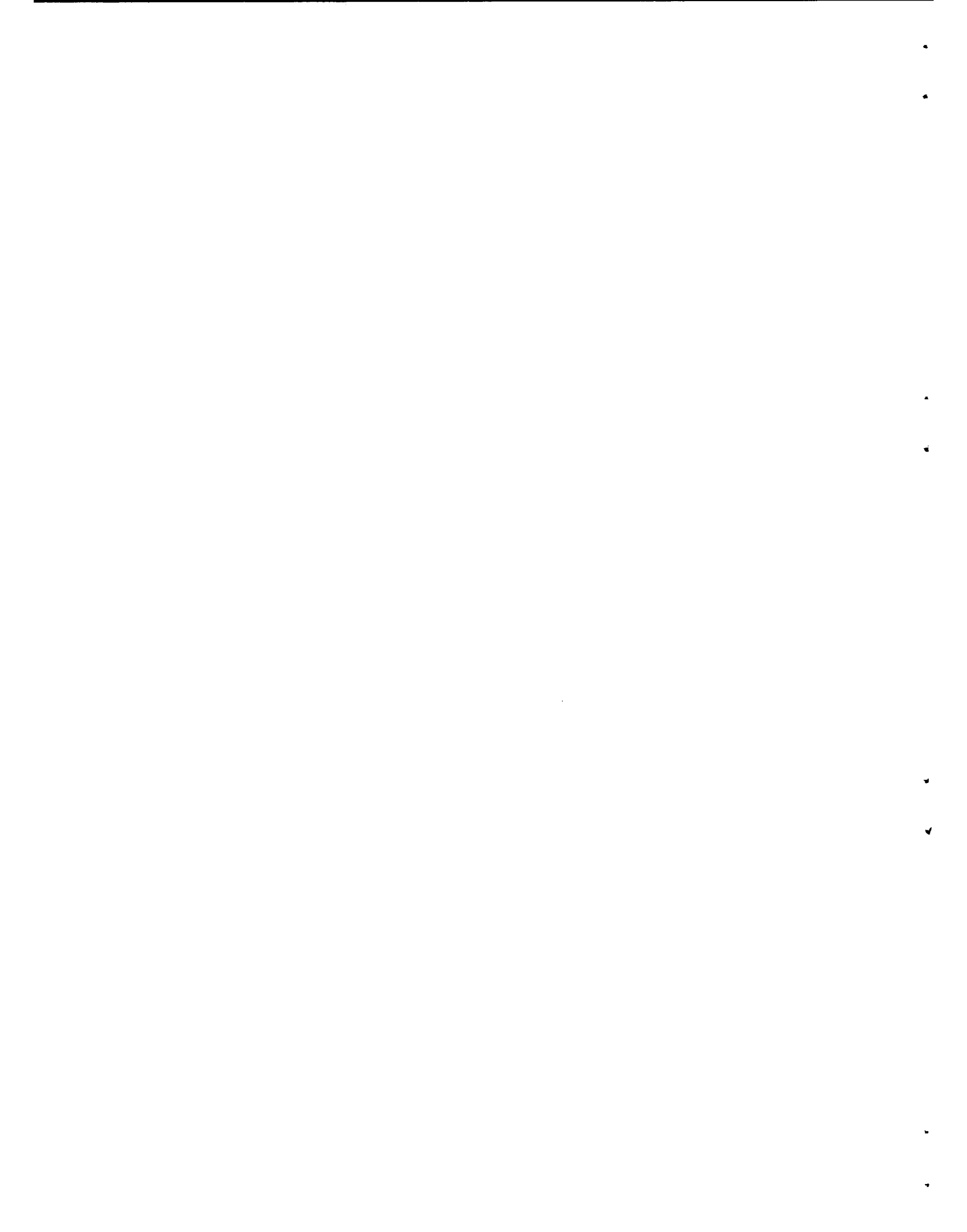
- Table 1. Summary of Existing Data on Pulse Height-Energy Relationship in Anthracene

LIST OF FIGURES

Figure	Page
1. Positive Beta Spectrum of Cu <sup>64</sup> and the Theoretical Slowing-Down Spectrum in Copper -----	8
2. Slowing-Down Time as a Function of Initial Positron Energy	10
3. Line Profile Due to Compton Absorption of Annihilation Radiation -----	16
4. Effect of Compton Absorption on a Continuous Positron Spectrum -----	17
5. Pulse Height (Channel Number) in Anthracene as a Function of Electron Energy for a Linear Relationship and According to Birks' Theory, With Both Curves Normalized to Agree at 624 keV -----	25
6. Expanded Section of Low Energy Portion of Fig. 5 -----	26
7. Intercept Energy as a Function of Electron Energy -----	28
8. Block Diagram of Positron Coincidence Spectrometer -----	31
9. Photomultiplier Load Circuit -----	33
10. Effect of Earth's Magnetic Field on Transmission of Positrons From Source to Detector -----	35
11. Sectional View of Spectrometer -----	36
12. Isomeric View of Copper Cavity Source -----	40
13. Decay Schemes of Cu <sup>64</sup> , Cs <sup>137</sup> , and Pm <sup>147</sup> -----	41
14. Dependence of Efficiency of NaI(Tl) Scintillation Spectrometer on Count Rate -----	44
15. (Cs-Ba) <sup>137</sup> Beta Spectrum Using Anthracene Crystal -----	47
16. Channel Number Versus Pulse Height For Pulse Height Analyzer	48
17. Fermi Plot of Pm <sup>147</sup> -----	51
18. Pulse Height Distribution for Annihilation Radiation in NaI(Tl) -----	53

LIST OF FIGURES(Con't)

Figure	Page
19. Positron Spectrum from Plane Source of $\text{Cu}^{64}$ in Copper.---	55
20. Beta-Gamma Spectrum and Gamma Spectrum from a Plane Source $\text{Cu}^{64}$ -----	57
21. Beta-Gamma Spectrum and Gamma Spectrum from A Cavity Source of $\text{Cu}^{64}$ -----	58
22. Experimental Positron Flux and the Continuous-Slowing-Down Theory -----	59



## INTRODUCTION

Knowledge of the spectral distribution of the primary and secondary electron flux generated in an infinite medium by ionizing radiation is of basic importance in understanding the effects of radiation on living matter.

Most measurements in the past on the deposition of energy from electrons in solids have been made either with an anisotropic situation or in a medium containing boundaries, e.g. secondary emission experiments or stopping power measurements in thin foils. In such cases, electron scattering tends to obscure the basic physical processes wherein the electron loses energy to the medium. If, however, a medium is chosen which is larger in size than the range of the highest energy electron present, and a vacuum cavity is introduced within this medium, the electron flux within the cavity is representative of the flux within the medium. Then if a channel connects the cavity with an electron spectrometer, a sample of this flux may escape into the electron spectrometer for energy analysis. The cavity source concept is similar to the concept of a black-body cavity with the substitution of electron flux for electromagnetic flux.

Birkhoff et al.<sup>1</sup> measured the spectral distribution of both primary and secondary electron flux inside a vacuum cavity in a

---

<sup>1</sup>R. D. Birkhoff, H. H. Hubbell, J. S. Cheka, and R. H. Ritchie, Health Physics 1, 27 (1958).

medium composed of  $P^{32}$  uniformly dispersed in bakelite with cavity walls thicker than the beta range. The measured flux compared favorably with the theoretical total flux above 0.35 MeV as calculated from the Spencer-Fano-Attix theory with a slight disagreement in the 0.05-to 0.35-MeV region which was not considered significant due to experimental uncertainties and approximations made in the evaluation of the theory.

In the present study, use of a positron emitter permitted the measurement of the primary component of the slowing down flux separately. This is possible because the positron retains its identity from birth until annihilation, whereas a primary electron is indistinguishable from a secondary of the same energy. Organic scintillators were used for the flux measurements, with anthracene being chosen because of its high relative pulse height, high efficiency for beta detection, and low gamma-ray response. It was also an obvious choice because previous research concerning its response to electrons provided correction factors for the slightly non-linear, pulse height-energy relationship.

The experimental method consisted of allowing positrons from a cavity source to strike and be absorbed in a thin anthracene crystal. After losing essentially all of their initial kinetic energy, the positrons were annihilated, and each emitted two 0.511 MeV gamma rays. A NaI(Tl) spectrometer placed near the anthracene crystal but shielded from the cavity source detected one of the oppositely directed annihilation gammas and electronically gated a

multichannel pulse height analyzer connected to the anthracene spectrometer if the annihilation gamma was detected under the photopeak in the NaI(Tl) spectrometer. The multichannel analyzer then allocated the coincident pulse produced by the anthracene spectrometer to a channel appropriate to the pulse size where it was stored as a count. After suitable corrections for nonlinearities in the anthracene pulse height-energy relationship, the primary slowing down spectrum was obtained.

## II THEORY

### A. Beta Spectra

#### 1. Continuous Slowing Down Theory

A beta particle born in an infinite, homogeneous medium with an energy  $E_i$  travels through the medium dissipating energy by inelastic nuclear collisions with the subsequent emission of bremsstrahlung and by excitation and ionization of atoms in the medium. The fraction<sup>2</sup> of the initial beta particle energy which is lost through radiative nuclear collisions as the particle slows to rest is approximately

$$\frac{\Delta E}{E_i} \simeq 0.0007 Z E_i \quad (1)$$

---

<sup>2</sup>R. D. Evans, THE ATOMIC NUCLEUS, (McGraw-Hill Book Co., Inc., New York, 1955) 617.

and the fractional<sup>3</sup> loss of energy in this manner by beta particles from a continuum is

$$\frac{\Delta E}{E_{av}} \approx \frac{Z}{3000} E_{max} \quad (2)$$

where  $E_{av}$  is the average beta energy and  $E_{max}$  is the maximum energy, and all energies are in MeV. For 650-keV beta particles in copper with  $Z = 29$ , this effect is small, so that the primary mode of energy loss is excitation and ionization of the medium.

A few general remarks may be made regarding the slowing-down process. A primary electron can lose up to one half its energy in a single collision, and a positron can lose its entire energy. The positron is unique in that it retains its identity throughout the slowing-down process, while an electron losing more than half its energy in a collision is thereafter denoted a secondary. Collisions in which a substantial fraction of the energy is transferred are known to be rare, however. Thus most secondary electrons are born with energies of less than 100 electron volts. In 1954 Spencer and Fano<sup>4</sup> published a theory of electron slowing-down which treated most of the secondaries on a continuous slowing-down model; i e. a primary electron is considered to lose energy in infinitesimal increments and therefore may be thought of as losing energy

---

<sup>3</sup>Ibid., p. 619.

<sup>4</sup>L. V. Spencer and U. Fano, Phys Rev. 93, 1172 (1954).

continuously; however large losses were included as a source of new "primary" electrons.

Although this description is not completely precise, it is not unrealistic since so few collisions result in large energy losses. Recently Schneider and Cormack<sup>5</sup> determined the flux spectrum using the Monte Carlo Technique to calculate collisional case histories of individual electrons. They found that the spectrum determined in this way was in very good agreement with the continuous slowing-down model.

If one considers a spherical probe with one  $\text{cm}^2$  cross sectional area in an infinite beta-radioactive medium, then the flux at energy  $E$  is defined as the number of beta particles per unit energy which cross the sphere per second from any direction with energies between  $E$  and  $E + dE$ . If one multiplies the flux,  $\phi(E)$ , by the energy increment,  $dE$ , and then by the stopping power,  $dE/dx$ , which is the spatial rate of energy loss, the result is the energy loss per  $\text{cm}^3$  per sec by electrons with energy in  $dE$ .

That is, the energy loss per  $\text{cm}^3$  per sec is:

$$\phi(E) \cdot dE \cdot dE/dx$$

with dimensions:

$$\frac{\#}{\text{cm}^2 \text{-sec-keV}} \cdot \text{keV} \cdot \text{keV/cm} = \frac{\text{keV}}{\text{cm}^3 \text{-sec}}$$

---

<sup>5</sup>D. O. Schneider and D. V. Cormack, Rad. Res. 11, 418 (1959).

In the continuous-slowing-down model, one neglects large energy losses and assumes that every electron born with energy greater than  $E$  will at some time during its life pass through energy  $E$  and will therefore contribute to the flux at this energy. In equilibrium conditions  $N(E)$  electrons per  $\text{cm}^3$  per sec are born with energies between  $E$  and  $E + dE$ , and all electrons with initial energies above  $E$  will pass through the energy interval  $dE$  at  $E$ . The energy deposition in the medium from these electrons as they pass through  $dE$  will be

$$dE \cdot \int_E^{E_{\max}} N(E) dE = \text{energy loss per cm}^3 \text{ per sec} \quad (3)$$

with dimensions:

$$\text{keV} \cdot \frac{\#}{\text{cm}^3 \text{-sec-keV}} \cdot \text{keV} = \frac{\text{keV}}{\text{cm}^3 \text{-sec}} \quad (4)$$

By equating Equation (3) and (4) and solving this identity for  $\phi(E)$ , one has a method for calculating the slowing-down flux in simplest approximation.

$$\phi(E) = \frac{\int_E^{E_{\max}} N(E') dE'}{\left(\frac{dE}{dx}\right)_E} \quad (5)$$

Copper  $^{64}$  emits positrons in an allowed distribution<sup>6</sup> with a maximum energy of 650 keV so that one may calculate the nuclear beta spectrum

---

<sup>6</sup>BETA-AND GAMMA-RAY SPECTROSCOPY, ed. Kai Siegbahn, (Interscience Publishers, Inc., New York, 315) 1955.

from the Fermi function tabulated in an NBS publication<sup>7</sup>. The flux,  $\Phi(E)$ , may be calculated by Equation (5) using the stopping-power as tabulated in NBS Supplement to Circular 577<sup>8</sup>. The nuclear beta spectrum and the theoretical slowing-down spectrum are shown together in Fig. 1 with the former spectrum normalized to unit area. Actually, if there is one positron born per  $\text{cm}^3$  per sec with probability given by the  $\text{Cu}^{64}$  spectrum in an infinite homogeneous copper medium, the total flux  $\Phi$ , at equilibrium and integrated over all energies will be 0.0139 positrons per  $\text{cm}^2$  per sec.

The stopping power,  $dE/dx$ , as calculated<sup>9</sup> from the Rohrlich-Carlson expression<sup>10</sup> has limitations, the most important of which is the lack of a theory of energy loss for electrons with energies comparable to those of the atomic electrons, i.e. below about 10 keV. The mean ionization energy,  $I$ , which appears in the stopping-power formula, is very difficult to calculate theoretically, and the most useful evaluations of  $I$  have been determined experimentally. Experimental data are meager below 50 keV.

---

<sup>7</sup>"Tables for the Analysis of Beta Spectra," NBS Applied Math. Ser. 13.

<sup>8</sup>"Energy Loss and Range of Electrons and Positrons", Supplement to NBS Circular 577, U. S. Department of Commerce.

<sup>9</sup>Ibid.

<sup>10</sup>F. Rohrlich and B. C. Carlson, Phys. Rev. 93, 38, 1954.

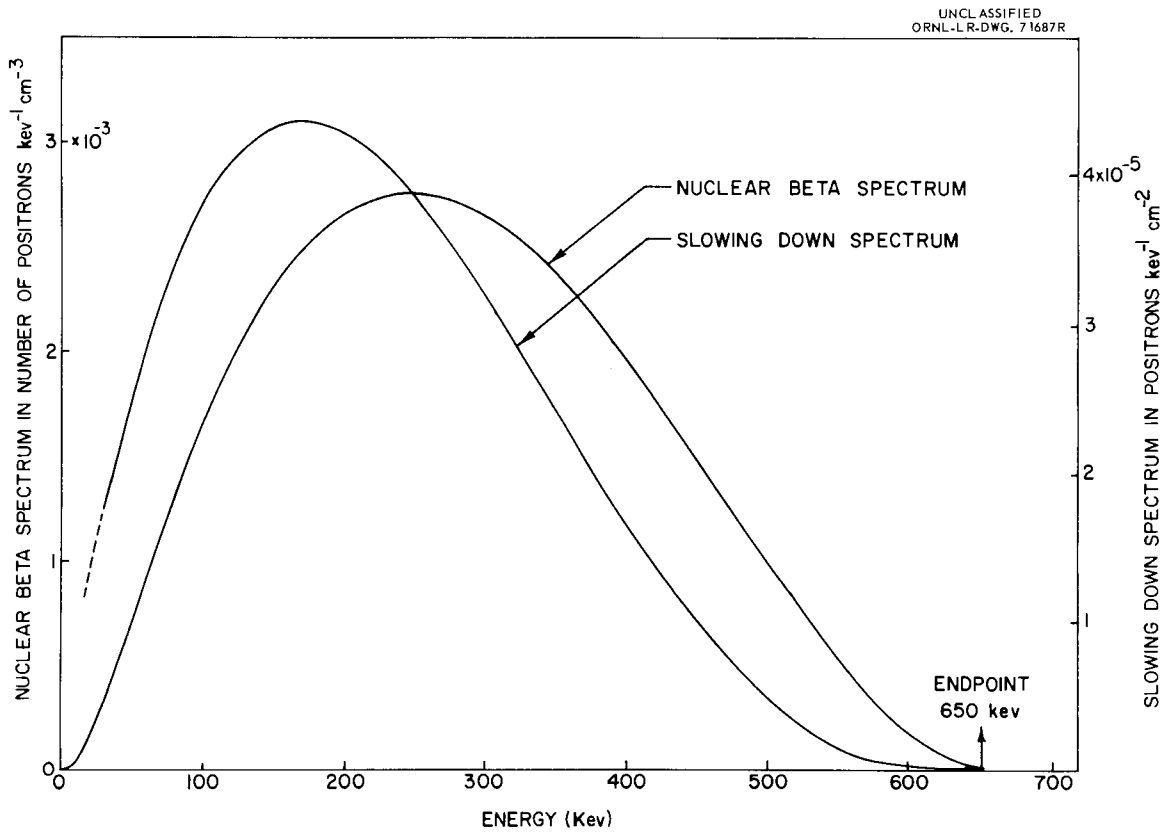


Fig. 1. Positive Beta Spectrum of  $\text{Cu}^{64}$  and the Theoretical Slowing-Down Spectrum in Copper.

Because anthracene is a fast phosphor with a decay time of about  $10^{-8}$  sec, it is instructive to calculate the slowing-down time for positrons in anthracene to see if the light pulse might be emitted substantially earlier than the annihilation radiation. A positron born with energy  $E$  in a medium slows down and eventually annihilates with an electron with the emission of 3,2,1, or no photons. The slowing-down time,  $t(E)$ , of a positron born with energy  $E$  may be calculated as follows. If  $v$  is the electron velocity, and

$$\begin{aligned} v &= dx/dt \\ dt &= dx/v \end{aligned} \quad (6)$$

or

$$dt = \frac{dE}{(dE/dx)v}$$

so that

$$t(E) = \int_0^E \frac{dE}{S(E)v} \quad (8)$$

where  $S(E)$  is the stopping power of the medium for positrons.

Figure 2 shows the slowing-down time as a function of initial energy. The slowing-down time for a 650-keV positron is about  $17.7 \times 10^{-13}$  sec and thus no delay between positron absorption in the anthracene and emission of annihilation radiation comparable to circuit time constants would be anticipated.

Wallace<sup>11</sup> has compiled a very comprehensive summary of positron

---

<sup>11</sup>P. R. Wallace, "Positron Annihilation in Solids and Liquids" SOLID STATE PHYSICS, Vol. 10. F. Seitz and D. Turnbull, Eds., (Academic Press, New York 1960).

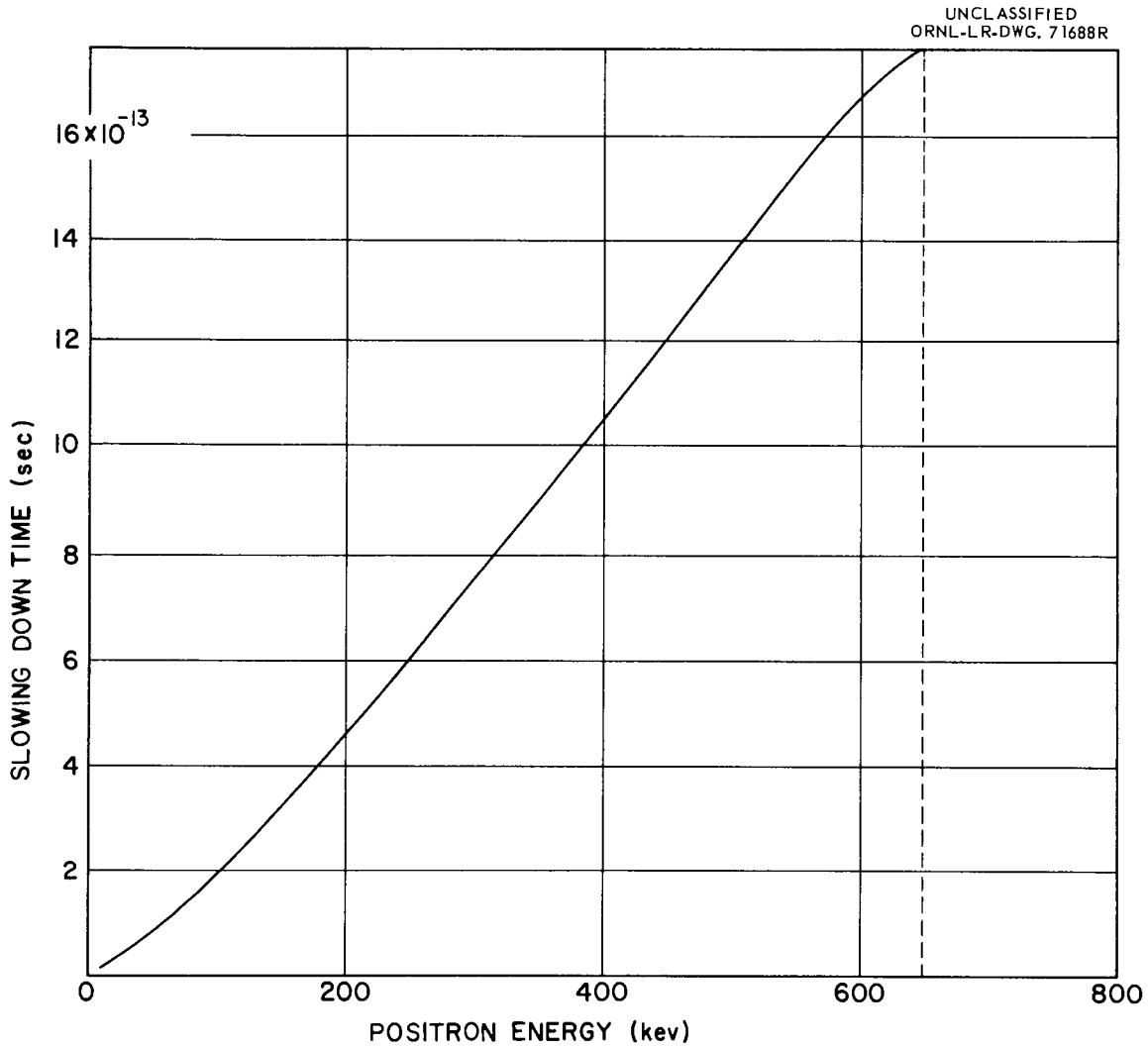


Fig. 2. Slowing-Down Time as a Function of Initial Positron Energy.

annihilation in solids and liquids, and positron annihilation in copper may be summarized as follows; positrons exhibit a single lifetime for annihilation of approximately  $1.2 \times 10^{-10}$  sec; there is virtually no annihilation in flight, and all the positrons thus become thermalized before annihilation; and virtually all the annihilation processes are accompanied by two photon emission. If annihilation in flight were a significant phenomenon, then the simple slowing-down theory would have to be modified to take it into account. Fortunately this is not the case.

## 2. The Effect of Coincident Pulses on Positron Spectra

Chance coincidences of  $\beta$ , X, or  $\gamma$  radiation pulses with a pulse from a positron absorption will cause a distortion of the observed spectrum which may be calculated from the average energy dissipation rate in the anthracene crystal. The total energy dissipation rate in the crystal at any time  $t$  is given by

$$R_E(t) = \int_0^{E_{\max}} E' N(E') dE'$$

where  $N(E')$  is the number of pulses from all radiations per unit time per unit energy at time  $t$  having energies between  $E'$  and  $E' + dE'$ . The average energy dissipated during a time interval between  $t$  and  $t + \tau$  is  $R_E(t)$  where  $\tau$  is a time of the order of the pulse duration of the crystal and the electronics. If  $R_E(t)$  is determined at time  $t_0$  and if the positron coincidence spectrum is measured between times  $t_1$  and  $t_2$ , then the average energy shift due to the chance coincidence background within a time  $\tau$  is

$$\bar{E} = \frac{\int_{t_1}^{t_2} R_E(t_0) \tau e^{-\lambda(t-t_0)} dt}{\int_{t_1}^{t_2} dt} \quad (11)$$

or

$$\bar{E} = \frac{R_E(t_0) \tau e^{-\lambda(t_1 - t_0)}}{\lambda(t_2 - t_1)} \left[ 1 - e^{-\lambda(t_2 - t_1)} \right] \quad (12)$$

Another spectral distortion is due to the partial absorption of one or both gamma rays from a positron annihilating in the anthracene. The coincidence technique discriminates in part against positron pulses which are thus enhanced in energy, because the photon absorbed in the NaI(Tl) crystal had to produce a pulse in this crystal under the photo-peak; i.e., the photon could not lose much energy (< 25 keV) in the anthracene or it would fail to gate the anthracene spectrometer. If one neglects this discrimination for the purposes of simplification, one can calculate the effect of these Compton interactions on the positron spectrum. The problem may be considered in three parts.

One must first have an estimate of the gamma ray path length in the anthracene crystal. Because a line between the thin anthracene button and the center of the sodium iodide crystal lies tangent to the face of the anthracene button, the problem of path length may be simplified to asking: what is the average chord length in a circle? A chord located at a distance  $x$  from the center of a

circle of radius  $r$ , has a length  $2\sqrt{r^2 - x^2}$  whose value, averaged over all values of  $x$ , is given by

$$\overline{\text{chord}} = \frac{1}{r} \int_0^r 2\sqrt{r^2 - x^2} dx = \frac{\pi r}{2} \quad (13)$$

For a crystal 0.5 inch in diameter, this length is 1.00 cm. It should be noted that the actual physical situation, wherein a positron annihilating at any point within the crystal fires oppositely directed .511-MeV gamma rays, is replaced in this calculation by a single .511-MeV gamma ray traversing an entire chord. Because of the short ranges of most of the positrons in the absorbing crystal, most of the annihilation will occur near the front face of the crystal with the result that the order of half of any track will be lost on the average. The actual track length will thus be taken as about 0.5 cm.

Next the average energy deposited in the anthracene by the annihilation gammas may be calculated. Positron pulses will be increased in size by the addition of this energy, and it is important to estimate the average size of this effect. The differential cross section per electron per keV,  $\frac{d\sigma}{dT}$ , for generating a secondary electron of energy  $T$  from a photon of energy  $E$  is given by the Klein-Nishina formula.<sup>12</sup> For .511-MeV photons this cross section varies only slightly

---

<sup>12</sup>National Bureau of Standards Circular 542, "Graphs of the Compton Energy Angle Relationships and the Klein-Nishina Formula from 10 keV to 500 MeV," Washington D. C., 84, 1953.

with energy over the Compton electron energy range from zero to 341 keV and may be taken as a constant value of  $7.7 \times 10^{-28} \text{ cm}^2 \text{ keV}^{-1}$ . The average Compton electron energy deposited in the anthracene per positron absorbed is:

$$\bar{T} = N_A \left(\frac{\bar{Z}}{A}\right) \rho t \left(\frac{\overline{d\sigma}}{dt}\right) \int_0^{341} T dT \quad (14)$$

where  $\left(\frac{\bar{Z}}{A}\right) = 0.53$ , and  $\rho = 1.25 \text{ g cm}^{-3}$  for anthracene, and  $t = 0.5 \text{ cm}$ . Substitution of these yields  $\bar{T} = 8.93 \text{ keV} \simeq 9 \text{ keV}$ . Clearly, a shift of pulse heights of this average value will produce an observable experimental error.

It would seem necessary to explore this effect in more detail. The total probability of interaction is given by the integral of the differential cross section over all electron energies:

$$P = N_A \left(\frac{\bar{Z}}{A}\right) \rho t \left(\frac{\overline{d\sigma}}{dt}\right) \int_0^{341} dT \quad (15)$$

For the same constants as before,  $P = .0524 \simeq .05$ . Thus 5% of all photons will liberate a Compton electron in the anthracene. This electron will have any energy between zero and 341 keV with almost equal probability.

During a counting interval,  $N(E)dE$  positrons of energies between  $E$  and  $E + dE$  are detected. In the absence of other distortions,  $0.95 N(E)dE$  will appear as a pulse height proportional to  $E$ , and  $0.05 N(E)dE$  will appear as pulses corresponding to energies between  $E$  and  $E + 341 \text{ keV}$ . The resulting line profile corresponding to

positrons of energy  $E$  is shown in Fig. 3.

The total spectral distribution  $N''(E)$  observed at energy  $E$  is the sum of the contributions from line profiles for all energies from  $E-341$  to  $E$ . Mathematically, the relationship between observed spectrum  $N''(E)$  true positron spectrum  $N(E)$  is:

$$N''(E) = 0.95 N(E) + 1.5 \times 10^{-4} \int_{E-341}^E N(E') dE' \quad (16)$$

or

$$N(E) = 1.05 \left[ N''(E) - 1.5 \times 10^{-4} \int_{E-341}^E N''(E') dE' \right] \quad (17)$$

where the observed spectrum has been substituted for the true spectrum under the integral for purpose of error calculations. The spectrum calculated from Eq. (16) and the continuous-slowing-down model as it would be observed considering this distortion alone is shown in Fig. (4) where it may be compared with the continuous-slowing-down spectrum in the absence of this distortion.

## B. Nonlinearities Inherent in the Scintillation Method

### 1. Crystal Nonlinearity

Bisi et al.<sup>13</sup> recognized the usefulness of anthracene scintillation techniques in beta-ray spectroscopy and measured the negative beta spectra of  $P^{32}$ ,  $W^{185}$ ,  $Co^{60}$ , and  $Tm^{170}$  in the energy

---

<sup>13</sup>A. Bisi, E. Germagnoli, and L. Zappa, Nuovo cimento (10) 3, 1007 (1956).

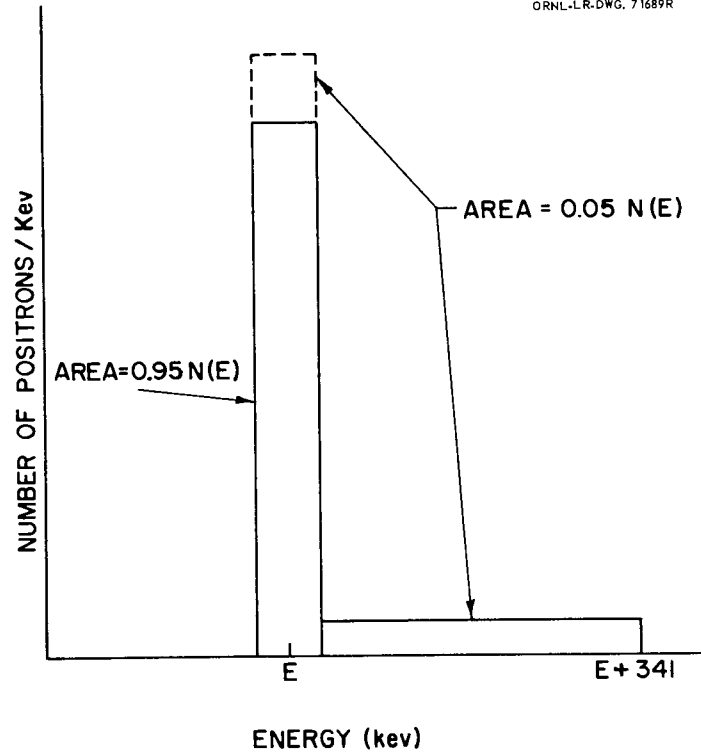
UNCLASSIFIED  
ORNL-LR-DWG. 71689R

Fig. 3. Line Profile Due to Compton Absorption of Annihilation Radiation.

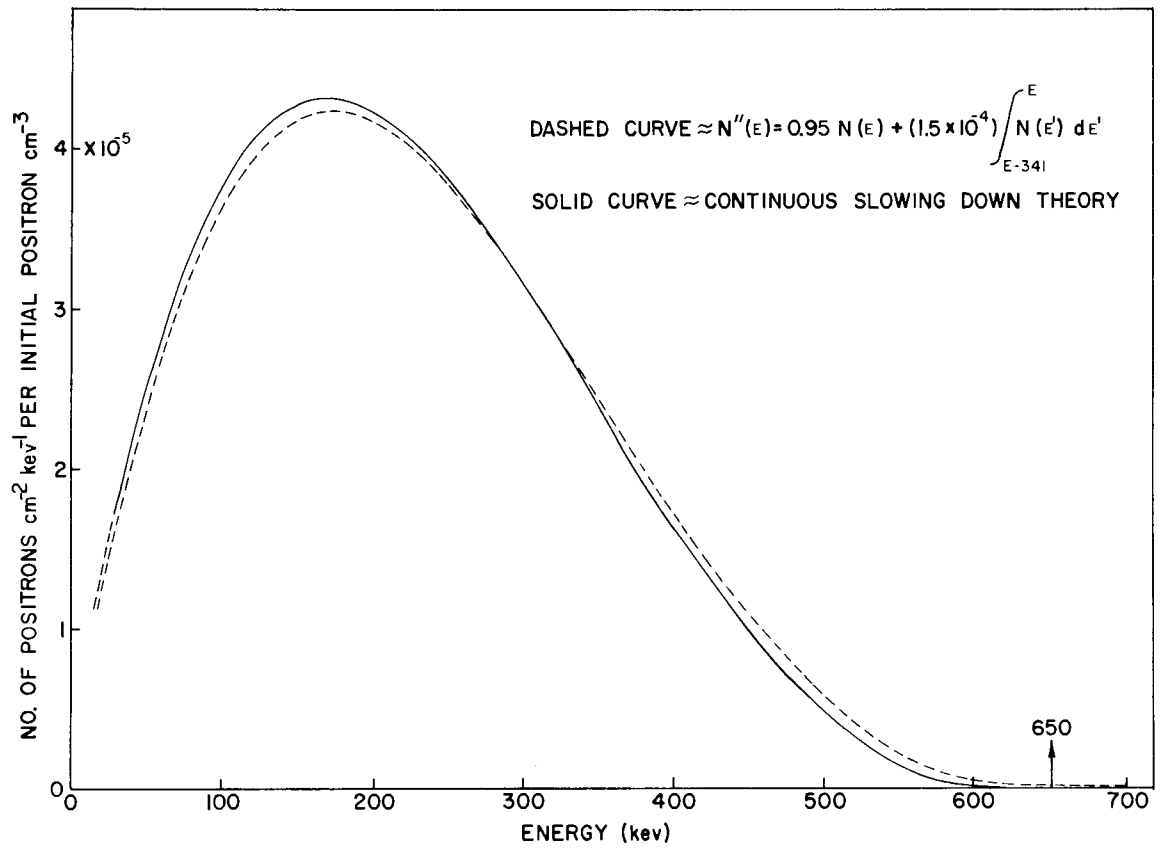
UNCLASSIFIED  
ORNL-LR-DWG. 71690R

Fig. 4. Effect of Compton Absorption on a Continuous Positron Spectrum.

ranges of 300 - 1640 keV, 100 - 420 keV, 60 - 320 keV, and 250 950 keV, respectively. They attributed a deviation in the Fermi plots of these spectra at energies less than one half the maximum energy to backscattering effects and used a hollow crystal spectrometer to minimize these effects. The beta spectrum of  $S^{35}$  from 20 keV to 160 keV has been measured by Hoffman<sup>14</sup> using an anthracene cleavage crystal spectrometer.

In 1959 Bhattacharjee et al.<sup>15</sup> used an anthracene crystal 1 cm thick by 4 cm diameter in their study of the decay scheme of  $Pm^{148}$ . They compared the spectral results using anthracene favorably with the spectra determined using a magnetic beta spectrometer.

Gubernator et al.<sup>16</sup> compared the anthracene response to surface incident electrons with the response to positrons and concluded that the light yield for positrons might be slightly below that of electrons, but the difference was less than 2%.

A summary of the data available from previous research on the response of the anthracene to monoenergetic electrons is presented in Table I. The nonlinear response of anthracene is

---

<sup>14</sup>K. W. Hoffman, Z. Physik 148, 303 (1957).

<sup>15</sup>S. K. Bhattacharjee, Baldev Sahai, C.V.K. Baba, Nuclear Physics, 12, 356 (1959).

<sup>16</sup>K. Gubernator, R. H. Heckmann and A. Flammersfeld, Z. Physik, 158, 268 (1960).

TABLE 1

## SUMMARY OF EXISTING DATA ON PULSE HEIGHT-ENERGY RELATIONSHIP IN ANTHRACENE

Observer	Source of Radiation	Crystal Thickness (cm)	Energy Range (keV)	Linearity of Energy Response and Remarks
Ramler and Freedman <sup>17</sup>	Electron gun	0.1 and 1.0	0 - 20	Observed a very rapid falloff of the relative counting efficiency (defined as peak counting rate divided by peak collector current in electrometer of $\beta$ -ray spectrometer) below 20 keV
Hopkins <sup>18</sup>	$\beta$ -ray	1.29	30 - 1900	Linear above 125 keV with 25 keV intercept and nonlinear below 125
Taylor et al. <sup>19</sup>	Electron gun	0.3	0.5 - 624	Linear above 100 keV and nonlinear below
Robinson and Jentschke <sup>20</sup>	K-capture X-rays	1	9 - 24	Linear within error

<sup>17</sup>W. J. Ramler and M. S. Freedman, Rev. Sci. Instr. 21, 784 (1950).

<sup>18</sup>Hopkins, loc. cit.

<sup>19</sup>C. J. Taylor et al., Phys. Rev. 84, 1034 (1951).

<sup>20</sup>W. H. Robinson and W. H. Jentschke, Phys. Rev. 95, 1414 (1954).

TABLE 1 -- Continued.

Observer	Source of Radiation	Crystal Thickness (cm)	Energy Range (keV)	Linearity of Energy Response and Remarks
Fowler and Roos <sup>21</sup>	X-ray tube	0.2	10 - 40	Linear within error
Birks and Brooks <sup>22</sup>	X-ray tube	0.2	6 - 30	Linear within error but noticed a difference between this response and the response to external electrons as observed by Taylor et al. <sup>9</sup>
Johnston et al. <sup>23,24</sup>	Electron gun	0.152	10 - 120	Linear function of energy with intercepts of 4.5 keV and 3.5 keV for thick and thin crystals, respectively
Gubernator et al. <sup>25</sup>	$\beta$ -ray spectrometer	0.022 0.3 2.0	25 - 200	Linear within error with an intercept of a few keV
von Schmeling <sup>26</sup>	Electron gun	0.02	1 - 12	Linear above 5 keV

<sup>21</sup>J. M. Fowler and C. E. Roos, Phys. Rev. 98, 996 (1955).<sup>22</sup>J. B. Birks and F. D. Brooks, Proc. Phys. Soc. (London) 69B, 721 (1956).<sup>23</sup>Johnston, loc. cit. <sup>24</sup>Johnston, loc. cit. <sup>25</sup>Gubernator, loc. cit.<sup>26</sup>H. H. K. B. von Schmeling, Z. Physik 160, 520 (1960).

most apparent at low energies as evidenced by studies listed. Hopkins<sup>27</sup> obtained an intercept of 25 keV by extrapolating the curve of pulse height vs. energy to zero pulse height from data in the 0.125-to 3.2-MeV range. In more recent work Johnston et al.<sup>28,29</sup> obtained a value of 4 keV by extrapolating from data taken below 120 keV. The latter work has been corroborated by Gubernator et al.<sup>30</sup> in their studies of anthracene response to beta particles of energies between 20 and 200 keV. These differing intercept energies and the apparent linearity of the pulse height-energy relationship may be explained with the aid of the theory of Birks<sup>31</sup> on the scintillation process as follows. Let S be the number of photons emitted by the scintillating crystal during the complete absorption of an energetic electron. In Birks' theory the spatial rate of production of photons along the electron track,  $dS/dx$ , depends on the spatial rate of energy loss or stopping power  $dE/dx$  as follows:

$$dS/dx = \frac{A \, dE/dx}{1 + (kB \, dE/dx)} \quad (18)$$

where A and B are constants of proportionality and k is the differential

---

<sup>27</sup>J. I. Hopkins, Rev. Sci. Instr., 22, 20(1951).

<sup>28</sup>L. W. Johnston, R. D. Birkhoff, J. S. Cheka, H. H. Hubbell and B. G. Saunders, ORNL-2298, 1959, ORNL, Oak Ridge, Tennessee.

<sup>29</sup>L. W. Johnston, R. D. Birkhoff, J. S. Cheka, H. H. Hubbell and B. G. Saunders, Rev. Sci. Instr., 28, 765 (1957).

<sup>30</sup>Gubernator, loc. cit.

<sup>31</sup>J. B. Birks, Proc. Phys. Soc., (London) A64, 874 (1951).

capture probability of a damaged molecule or quencher relative to an undamaged molecule or fluorescer. The constant A may be identified with the light producing efficiency of electrons in anthracene and  $k_B$  is related to the effective local quenching.<sup>32</sup> The range energy relationship of electrons has been studied by Glocker<sup>33</sup>, Libby,<sup>34</sup> and by Lane and Zaffarano,<sup>35</sup> and according to them the range,  $x$ , in  $\text{g cm}^{-2}$  is related to the electron energy  $E$  in MeV by the expression

$$x = bE^{5/3} \quad (19)$$

where  $b$  is a proportionality constant, and the expression holds for energies between 1 and 300 keV. This relationship may be differentiated and substituted into Equation (18) to obtain the differential fluorescence efficiency.

$$dS/dE = \frac{A}{\left[1 + (3k_B/5b)E^{-3/2}\right]} \quad (20)$$

Birks obtained an experimental value of 7.15 cm air per MeV for  $k_B$ , and the average value of  $b$  from the references listed is  $0.65 \text{ g/cm}^2(\text{MeV})^{-5/3}$ . One may then evaluate the quantity  $\alpha = 3k_B/5b$

---

<sup>32</sup>E. Newman, A. M. Smith, and F. E. Steigert, Phys. Rev., 122, 1520 (1961).

<sup>33</sup>R. Glocker, Z. Naturforsch 3a, 147 (1948).

<sup>34</sup>W. E. Libby, Analytical Chemistry 19, 2 (1947).

<sup>35</sup>R. O. Lane and D. J. Zaffarano, "Transmission of 0-50 Kilovolt Electrons by Thin Films with Applications to Beta-Ray Spectroscopy," Iowa St. Col. 439, (Dec. 1953).

$$\alpha = \frac{3 \times 7.15 \frac{\text{cm air}}{\text{MeV}} \times 0.001293 \frac{\text{g/cm}^2}{\text{cm air}} \times \frac{273}{288} \times (1000 \frac{\text{keV}}{\text{MeV}})^{2/3}}{5 \times 0.65 \frac{\text{g/cm}^2}{(\text{MeV})^{5/3}}}$$

$$= 0.81 (\text{keV})^{2/3} \quad (21)$$

The number of photons, S, may then be found immediately by integrating<sup>36,37</sup> Equation (20) and making the substitution for  $\alpha = 3kB/5b$ ; thus

$$S = AE \left[ 1 - \frac{3}{\mu^2} + \frac{3}{\mu^3} \tan^{-1} \mu \right] \quad (22)$$

where

$$\mu = E^{1/3} \alpha^{-1/2} \quad (23)$$

Fig. 5 shows S as a function of E under two different assumptions. Actually the ordinate here is the channel number of a multichannel analyzer into which the pulse from the photomultiplier is directed for analysis and storage. The function of the photomultiplier is to convert the number of photons S from the anthracene into a number of electrons proportional to S, and amplify this number of electrons. The circuitry connecting the photomultiplier and multichannel analyzer converts these electrons into a voltage pulse of amplitude proportional to S and shape- and duration-tailored to the requirements of the multichannel analyzer as discussed in Section III. Thus here

---

<sup>36</sup>Johnston, loc. cit.

<sup>37</sup>Health Physics Division Annual Progress Rept. 1959, ORNL-2806, 153.

and henceforth, channel number is to be interpreted as equivalent to number of photons emitted by the irradiated anthracene crystal. The upper curve of Fig. 5 represents a linear pulse height-energy relationship passing through the origin, and channel 250,  $E = 624$  keV (the  $\text{Ba}^{137}$  K-conversion energy). The lower curve is a plot of Equation (22) with the constant  $A$  adjusted so that this curve passes through this same upper point. Fig. 6 is an expanded portion of Fig. 5. The setting of channel 250 as equivalent to 624 keV is arbitrary and may be varied during the experiment by varying the amplification of the system.

At high energies the sum of the second and third terms in the bracket in Equation (22) approaches zero and

$$S \rightarrow AE \quad (24)$$

Thus a quantitative explanation is obtained for the apparent linear response of anthracene to high electron energies.

A quantitative expression<sup>38</sup> for the energy intercept may be obtained in the following way. The energy intercept  $E_i$  of the tangent to the pulse-height energy curve at some point  $(S_1, E_1)$  is given by

$$E_i = E_1 - S_1 \left[ \frac{dS}{dE} \right]_{E_1}^{-1} \quad (25)$$

If Equation (21) for  $dS/dE$  is substituted in Equation (25), then

---

<sup>38</sup>Ibid.

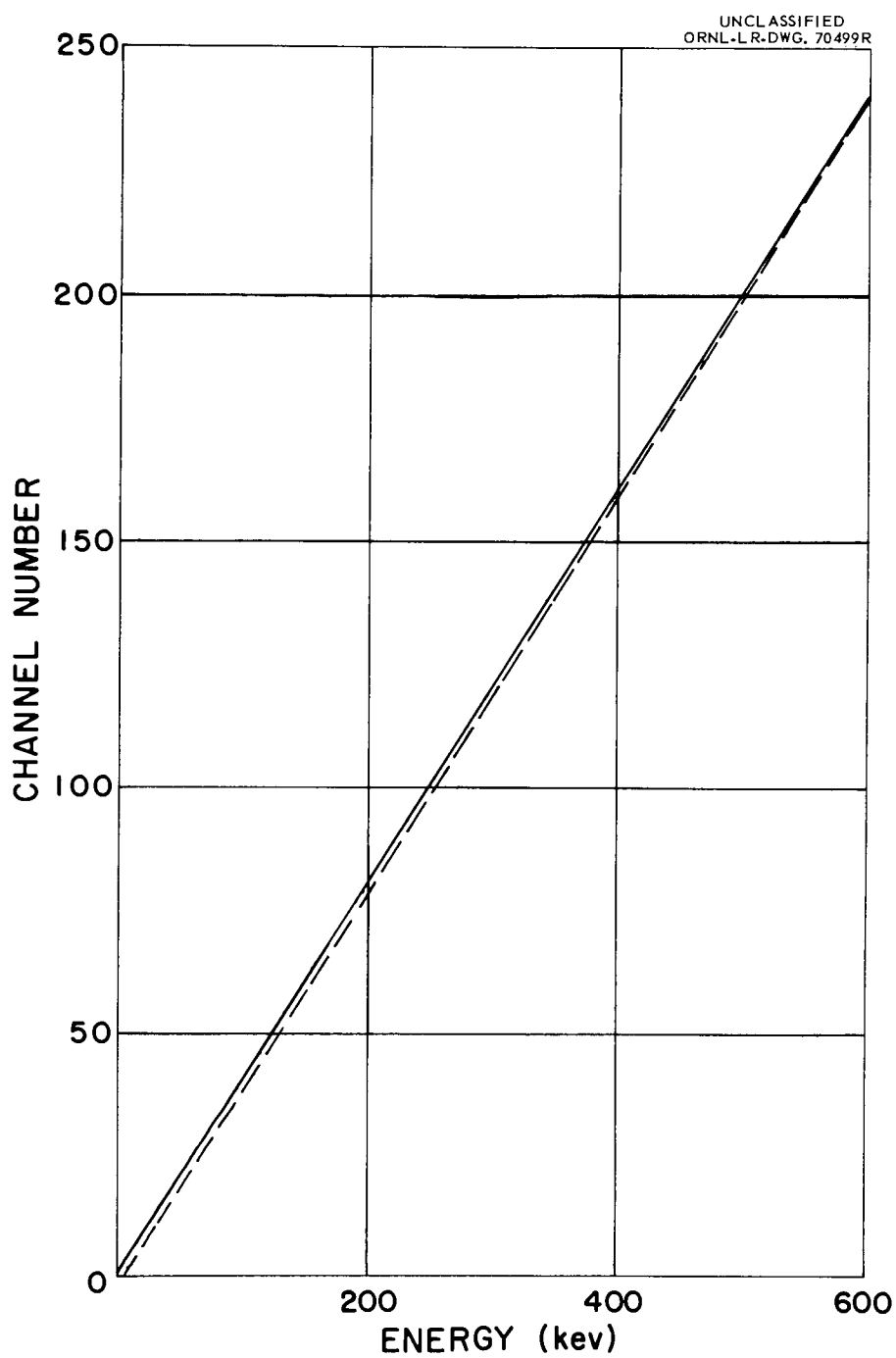


Fig. 5. Pulse Height (Channel Number) in Anthracene as a Function of Electron Energy for a Linear Relationship and According to Birks' Theory, With Both Curves Normalized to Agree at 624 keV.

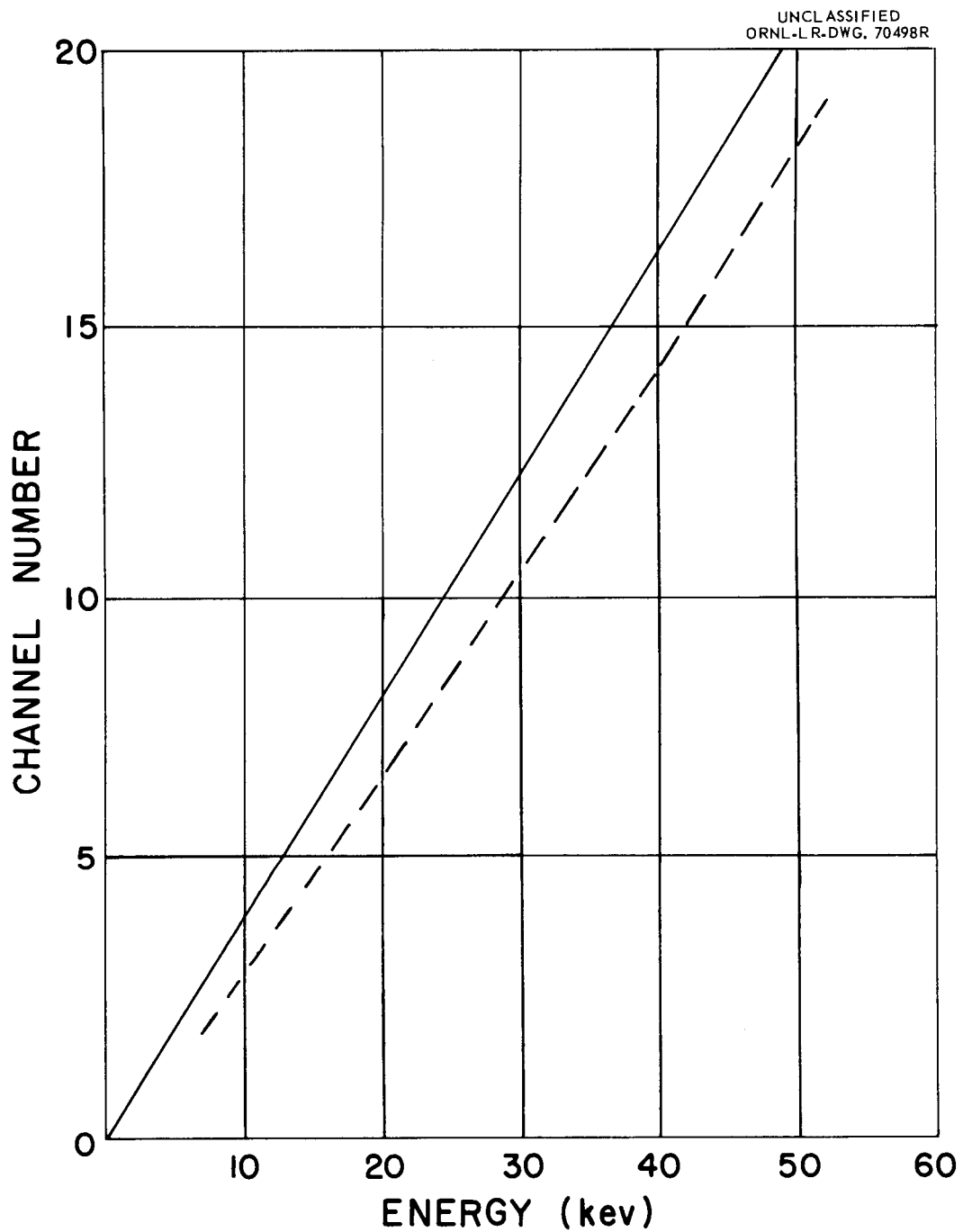


Fig. 6. Expanded Section of Low Energy Portion of Fig. 5.

$$E_i = E_1 \left\{ 1 - \left[ 1 + \mu_1^{-2} \right] \left[ 1 - e\mu_1^{-2} (1 - \mu_1^{-1} \tan^{-1} \mu_1) \right] \right\} \quad (26)$$

where  $\mu_1 = E_1^{1/3} \alpha^{-1/2}$ . A plot of this equation is shown in Fig. 7 for  $\alpha = 1 \text{ (keV)}^{2/3}$ .

At around 50 keV, the intercept is approximately 4 keV as found by Johnston et al.<sup>39</sup> and Gubernator<sup>40</sup> et al. However, if the slope is evaluated around 1.5 MeV,  $E_i$  is about 20 keV in good agreement with Hopkins.<sup>41</sup>

Newman et al.<sup>42</sup> point out that although Birks' simple model for fluorescent response discussed above is not completely adequate to explain the scintillation response to all charged particles, the experimental response is compatible with Birks' theory in "the so-called linear regions."

## 2. Bandwidth Correction

The bandwidth correction should be made whenever a nonlinearity is evident in the pulse-height energy response. This correction may be understood by considering the identity

$$N(E) dE = N_1(C) dC \quad (27)$$

where E and C are the electron kinetic energy and pulse height measured by analyzer channel number, respectively,  $N(E) dE$  is the

---

<sup>39</sup>Johnston, loc. cit.

<sup>40</sup>Gubernator, loc. cit.

<sup>41</sup>Hopkins, loc. cit.

<sup>42</sup>E. Newman, A. M. Smith, and F. E. Steigert, Phys. Rev. 122, 1520 (1962).

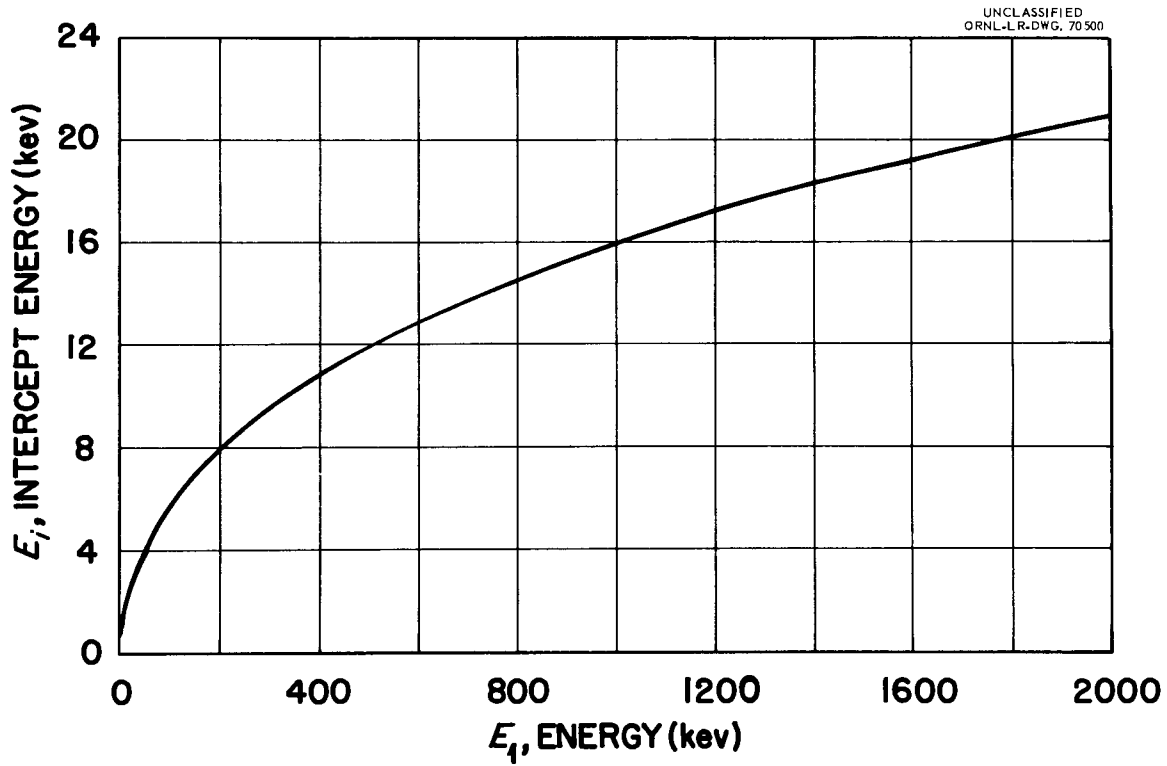


Fig. 7. Intercept Energy as a Function of Electron Energy.

number of electrons absorbed in anthracene having energies between  $E$  and  $E + dE$ , and  $N_1(C)dC$  is the number of counts appearing in channel  $C$  in the multichannel analyzer as a result. If the fluorescence efficiency of anthracene were a linear function of energy and the analyzer response were a linear function of photomultiplier pulse height, then the number of counts recorded in any channel could be interpreted directly as a number of electrons detected in a given energy interval. This is generally not the case with scintillators as discussed in the previous section; i e.  $dE/dC$  is not a constant but a function of  $E$ . As the slope of the response curve in Fig. 6 decreases at lower energies, the effective energy window,  $\Delta E$ , associated with one channel of width  $\Delta C$  increases, and the number of counts recorded will be artificially raised. One may relate the number of counts appearing in the analyzer channels,  $N_1(C)$ , to the number of electrons detected per unit energy,  $N(E)$  by

$$N(E) = N_1(C) \, dC/dE \quad (28)$$

by using the slope of the  $C$  vs.  $E$  response curve. Thus any point on a pulse height spectrum must be corrected in abscissa by use of Figs. 5 and 6 and in ordinate by Equation 28 before it may represent a point on the energy spectrum.

## III. ELECTRONIC APPARATUS

The photomultipliers used in this research were of type RCA 6199 with 10 stages, and 1.25-inch cesium-antimony semitransparent cathodes. The small cathode with S-11 type response is particularly suitable for anthracene which fluoresces with a wavelength of  $4400 \text{ \AA}$  at maximum emission. These tubes were operated at 750 volts as supplied by an Atomic Instrument Company Model 312 high voltage supply. In order to reduce the 60 cycle ripple voltage, the output was filtered by an R-C, T type filter of two  $270 \text{ K}\Omega$  resistors and a  $1 \text{ }\mu\text{f}$  capacitor to ground. The voltage was monitored by a Sensitive Research electrostatic voltmeter. The anthracene crystals were supplied by the Harshaw Chemical Company and were  $1/2$  inch in diameter and 2 mm thick.

The vacuum system consisted of a Welch Manufacturing Company Duo Seal vacuum forepump, a Consolidated Vacuum Corporation diffusion pump, and a liquid nitrogen cold trap.

A Nuclear Data Model ND101 Readout Unit was used to analyze the scintillation pulse height spectra as amplified by a Nuclear Data Model 500 Dual Amplifier-Discriminator. A Tektronix type 543 oscilloscope and an IBM electric typewriter were used in conjunction with the readout unit.

A mercury relay pulse generator, ORNL Model Q-1212D-IROC, was used to calibrate and examine the response of the analyzer.

Fig. 8 shows a block diagram of the circuitry as used for the positron coincidence measurements. In order for the Dual Amplifier

UNCL ASSIFIED  
ORNL-LR-DWG. 71691R

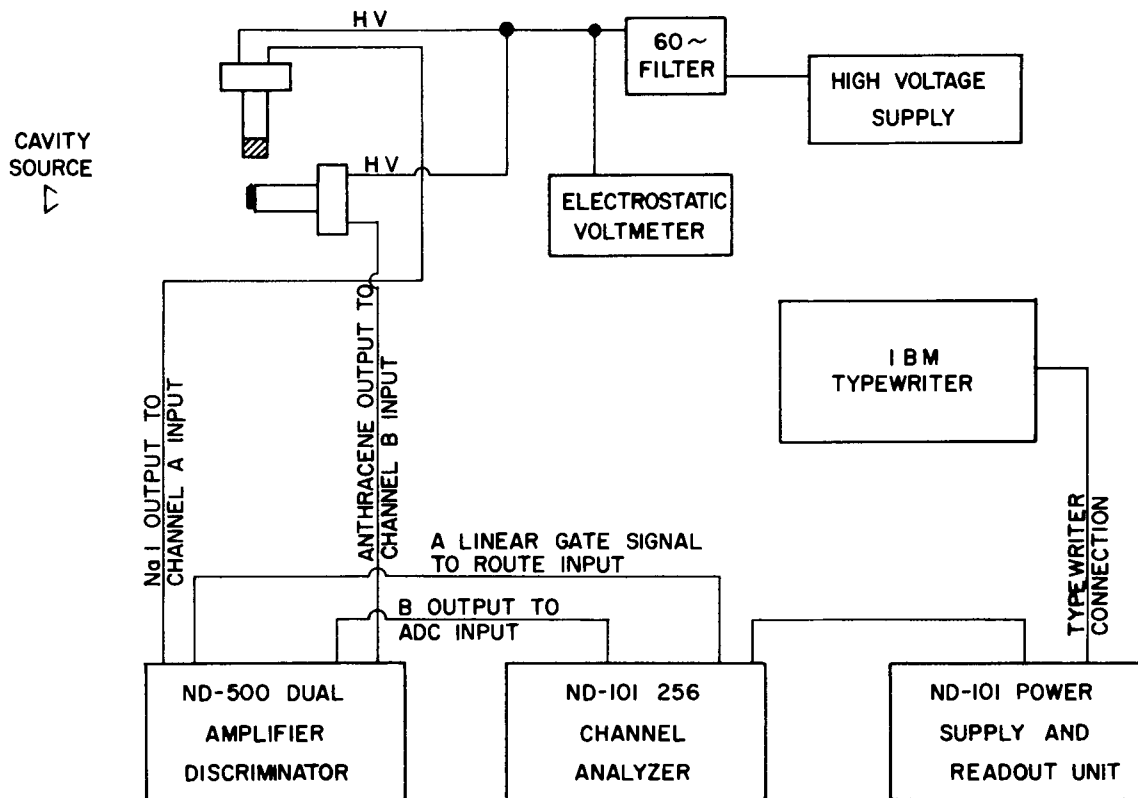


Fig. 8. Block Diagram of Positron Coincidence Spectrometer.

to operate properly, the pulse from the photomultipliers must have a decay time constant of between 30  $\mu$  sec and 50  $\mu$  sec. This was accomplished by adjusting the anode load resistance and the bypass capacitor and cable length to the values shown in Fig. 9. A diode circuit was also necessary to protect the amplifier input transistors from excessive back biasing by bypassing any positive transient pulses. This is also shown in Fig. 9. The voltage pulse appearing at the amplifier input was:

$$dE = \frac{dQ}{C_{\text{eff}}} \quad (29)$$

where  $Q$  is the charge collected by the photomultiplier anode and  $C_{\text{eff}}$  is:

$$C_{\text{eff}} = C_s + \frac{C_B \times C_c}{C_B + C_c} \quad (30)$$

$$C_{\text{eff}} \cong 37 \mu\mu\text{f} \quad (31)$$

The pulse time constant was:

$$\tau = R_{\text{eff}} C_{\text{eff}} \quad (32)$$

$$\tau \cong 30 \mu \text{ sec} \quad (33)$$

$$\begin{aligned} R_{\text{eff}} &= \frac{R_L \times R_c}{R_L + R_c} \\ &= 0.83 \text{ Megohm} \end{aligned} \quad (34)$$

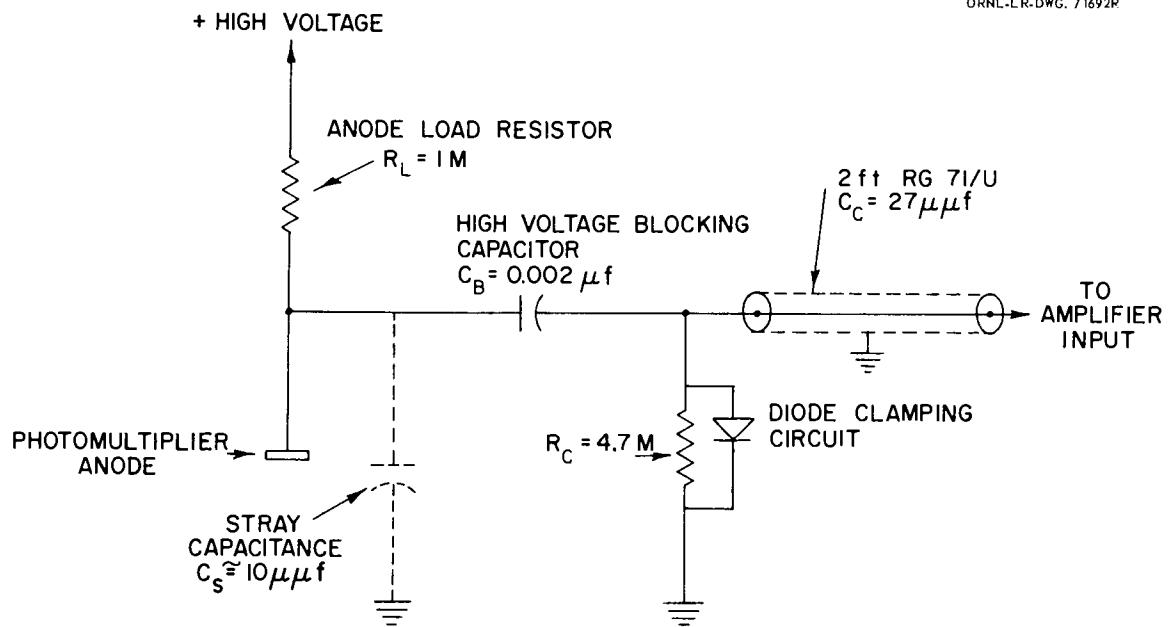
UNCLASSIFIED  
ORNL-LR-DWG. 71692P

Fig. 9. Photomultiplier Load Circuit.

## IV. ANTHRACENE SPECTROMETER

## A. Construction

The spectrometer was constructed in such a manner as to permit its use in a positron annihilation-gamma coincidence circuit. It was found necessary to separate the source from the anthracene crystal to remove the excessive gamma background in the NaI(Tl) crystal caused by the positrons which did not escape the source.

It was then necessary to determine the optimum source-to-crystal distance, i e., the distance which would provide the maximum shielding of the NaI(Tl) crystal but would not cause the loss of any low energy positrons. A measurement was made of the positron transmission through a tube, 0.75 inch diameter, and the results are shown in Fig. 10. The positrons traversing the tube struck a lucite disc and were annihilated. A fixed fraction of the annihilation gammas was detected with a NaI(Tl) crystal oriented to view the anthracene disc. A source-to-anthracene crystal distance of 12 inches was thought to cause no significant loss of low energy positrons due to deflection by the earth's magnetic field. It is of interest to note that Madansky and Rasetti<sup>43</sup> were unable to detect any positrons with energy less than 150 eV escaping the surface of a copper-64 source.

Fig. 11 shows a diagram of the spectrometer which consisted of a vacuum-tight aluminum tube with an anthracene crystal 0.5 inch

---

<sup>43</sup>L. Madansky and F. Rasetti, Phys. Rev. 79, 397 (1950).

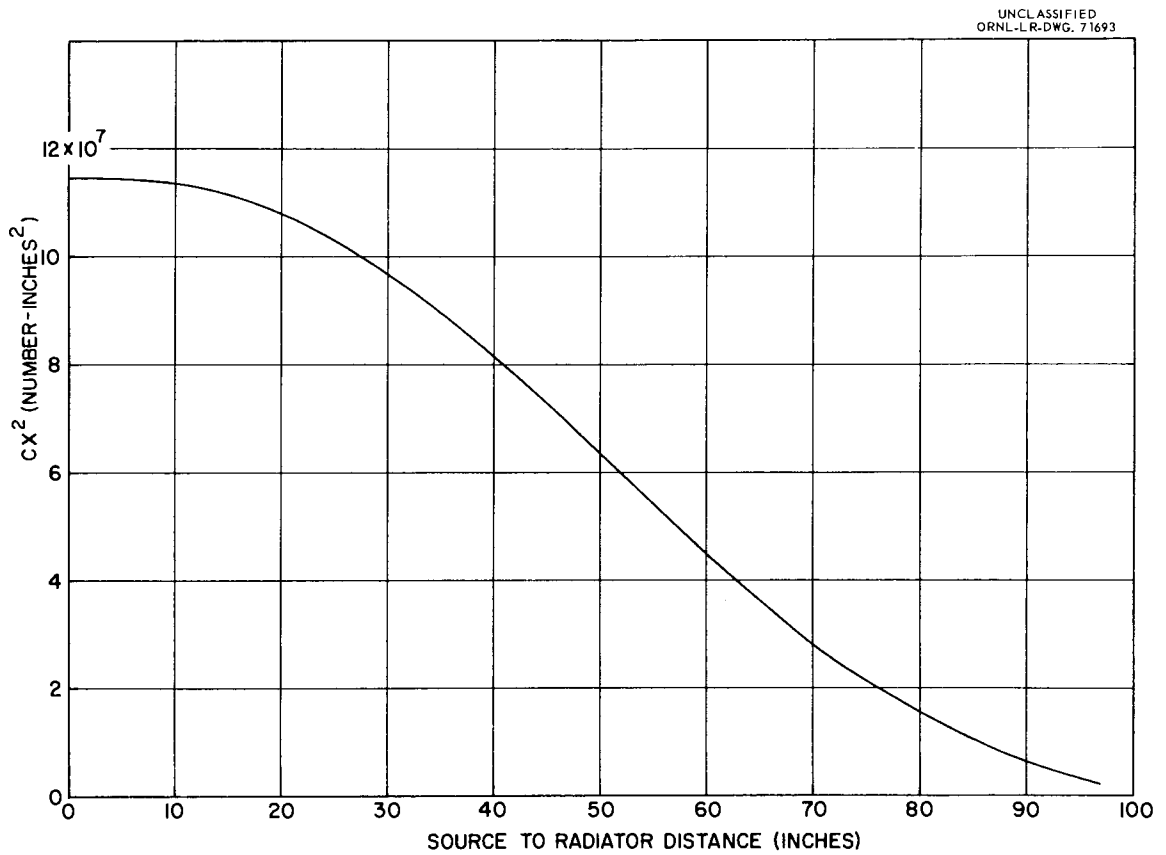


Fig. 10. Effect of Earth's Magnetic Field on Transmission of Positrons From Source to Detector.

UNCLASSIFIED  
ORNL-LR-DWG. 69824

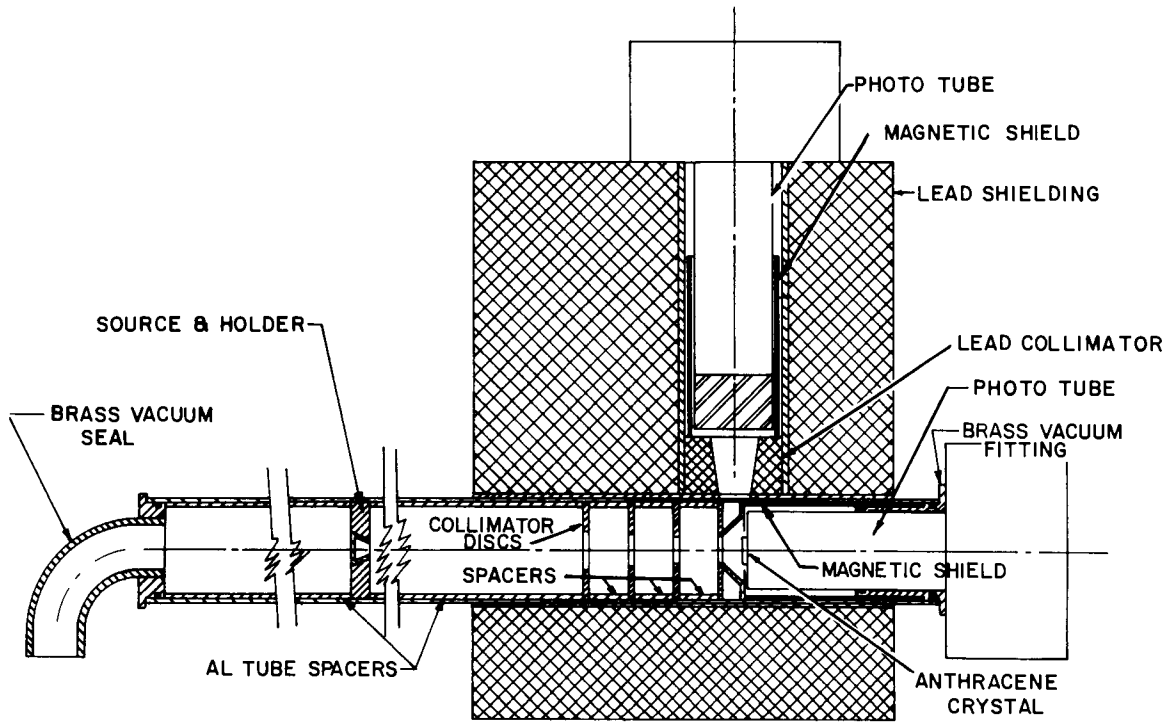


Fig. 11. Sectional View of Spectrometer.

diameter x 0.08 inch thick mounted on an RCA-6199 phototube with Dow Corning silicone grease for adhesion and good optical contact. A conical reflector with the apex removed was used to increase the optical efficiency of the system. The NaI(Tl) crystal was mounted on another RCA-6199 phototube and oriented perpendicular to the spectrometer axis so as to detect positron annihilations in the anthracene crystal. The NaI(Tl) crystal was shielded by lead. Lucite collimators produced a well defined beam of beta radiation from the sources to the anthracene. These were placed so as to minimize the solid angle subtended at the crystal for scattered beta particles. No lead was used in the aluminum tube either as shielding or as collimation in order to lessen the probability of an anthracene interaction with a lead x-ray produced by the annihilation radiation.

#### B. Source Preparation

##### 1. Barium-137

A bare barium-137 source was prepared by depositing a drop of radioactive solution on a 1 mil thick aluminum foil and drying it under a heat lamp. The solution was obtained from the Isotope Division of the Oak Ridge National Laboratory in the form of CsCl in HCl. The concentration was 1.25 mc/ml and the normality of the solution was 1.09 acid. The 624-keV internal conversion electrons from this source were used to calibrate the anthracene crystal by establishing one point on the pulse-height energy curve.

2. Promethium<sup>147</sup>

A Pm<sup>147</sup> beta source was prepared by drying a drop of radioactive solution on a thin formvar film on which a thin strip of aluminum had been vacuum evaporated to prevent the electrostatic charging of the source from affecting the energy spectra of the electrons. The formvar film was prepared by dissolving 100 mg of formvar 15/95 resin from Shawinigan Products Corporation in 18 ml of 1, 2 dichloroethane and allowing a drop of this warmed solution to spread out on the cleaned surface of cool, distilled water in a crystallizing dish. The edge of the dish was coated with a layer of beewax whose hydrophobic properties permitted the water level to extend above the edges of the dish. The surface of the water was cleaned by drawing a glass rod across the water in a scraping manner immediately before dropping the formvar solution on the water. The formvar was mounted on an aluminum disc 2 inches in diameter and 9 mils thick, with a 3/8-inch hole in the center. The edge of the disc was lifted vertically from the water in order to mount the formvar film. The formvar film was about 5  $\mu\text{g}/\text{cm}^2$  thick and the 1/16-inch-wide aluminum strip was about 10  $\mu\text{g}/\text{cm}^2$  thick. The Pm<sup>147</sup> was obtained from the Isotope Division at ORNL in the form of PmCl<sub>3</sub> in HCl. The solution was 0.19 N acid and the concentration was 24.81 mc/ml. This source was used to demonstrate the validity of Birks' theory of the scintillation process as it affects the efficiency of anthracene as a function of electron energy.

## 3. Copper -64

Fig. 12 shows an isometric view of the copper cavity source and holder. The holes in the latter were to improve pumping speed of the vacuum system. The fractional solid angle subtended at the base of the cone by the aperture in the cone was 0.10. The walls of the cavity were 0.018 inches thick and therefore infinitely thick to 650-keV positrons whose range in copper is  $369 \text{ g/cm}^2$ <sup>44</sup> or 0.0164 inches. The cavity source was irradiated in a  $6.5 \times 10^{11} \text{ n/cm}^2/\text{sec}$  thermal neutron flux in the Oak Ridge Graphite Reactor. Naturally occurring copper is composed of 69.1% Cu<sup>63</sup> and 30.9% Cu<sup>65</sup>, and therefore the radioisotopes Cu<sup>64</sup> and Cu<sup>66</sup> were produced by the reactions



The thermal activation cross sections<sup>45</sup> for these reactions are 4.5 barns and 1.8 barns, respectively. The Cu<sup>66</sup> decays with a half live of 5.1 minutes; and if spectral measurements are initiated after a decay time of the order of one hour, the Cu<sup>66</sup> activity remaining is a factor of 1000 less than its original value. Fig. 13 shows the modes of decay of Cu<sup>64</sup>.

The number of positrons born per  $\text{cm}^3$  per sec may be determined

---

<sup>44</sup>National Bureau of Standards, loc. cit.

<sup>45</sup>D. J. Hughes and R. B. Schwartz, Neutron Cross Sections, 2n ed., (Brookhaven National Laboratory, Upton) p. 8 (1958).

UNCLASSIFIED  
ORNL-LR-DWG. 71694

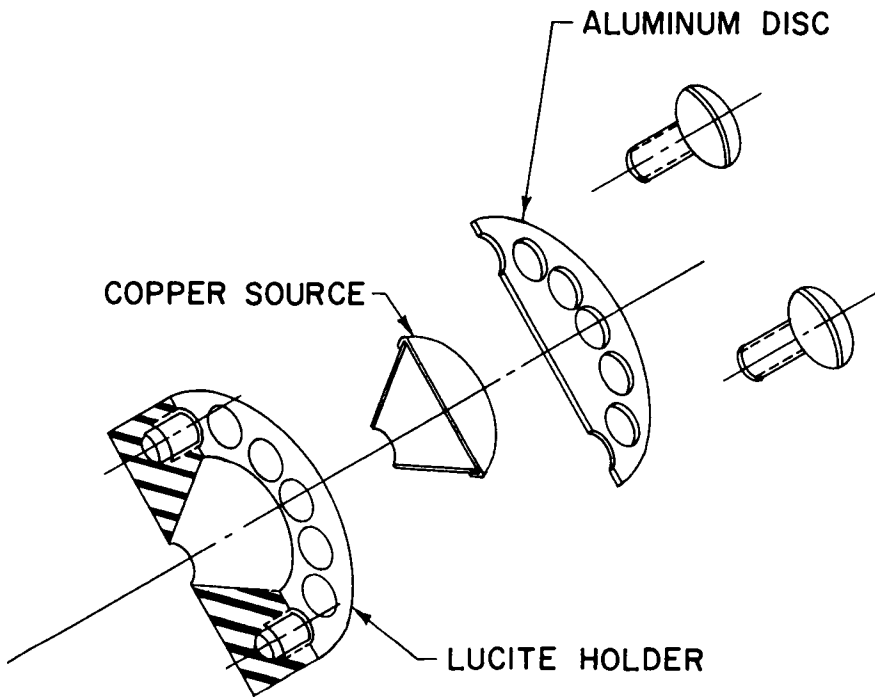
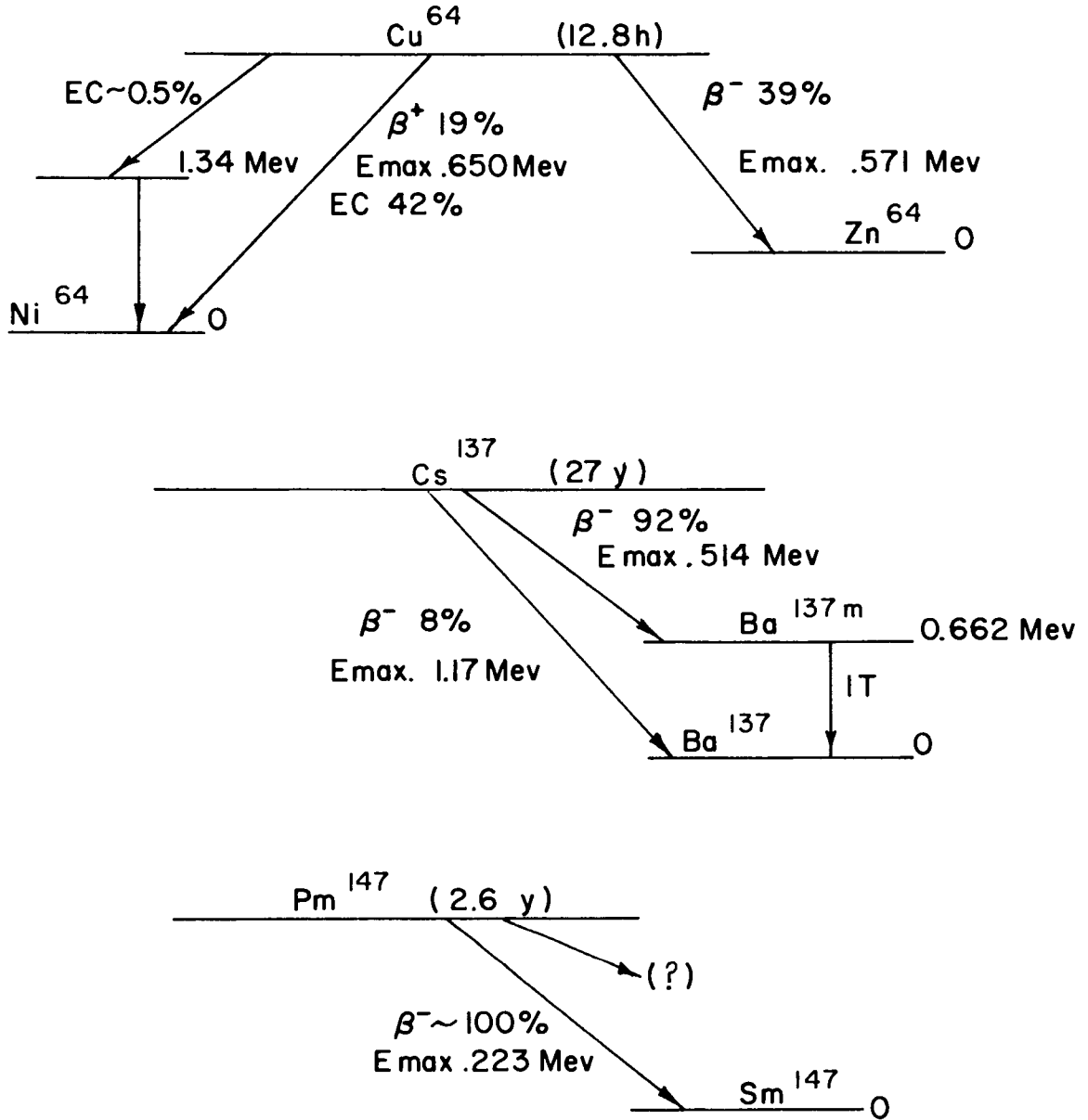


Fig. 12. Isomeric View of Copper Cavity Source.

UNCLASSIFIED  
ORNL-LR-DWG. 71695Fig. 13. Decay Schemes of Cu<sup>64</sup>, Cs<sup>137</sup>, and Pm<sup>147</sup>.

by activation calculations as follows. The differential equation for the rate of change of the number of  $\text{Cu}^{64}$  atoms per  $\text{cm}^3$  per sec is:

$$\frac{dN_{64}}{dt} = -N_{64}\lambda + \Sigma\phi \quad (37)$$

where  $\phi$  is the thermal neutron flux in neutrons per  $\text{cm}^2$  per sec and  $\Sigma$  is the macroscopic absorption cross section in  $\text{cm}^{-1}$ . The macroscopic cross section is equal to,  $N\sigma$ , the number of  $\text{Cu}^{63}$  atoms per  $\text{cm}^3$  multiplied by the microscopic absorption cross section in  $\text{cm}^2$ .

Equation (37) is easily solved to obtain:

$$N_{64} = \frac{\Sigma\phi}{\lambda} (1 - e^{-\lambda t}) \quad (38)$$

If the copper is removed from the reactor after an irradiation time  $T$ , the activity at a time  $t$  after removal is:

$$\frac{dN_{64}}{dt} = -\Sigma\phi(1 - e^{-\lambda T})e^{-\lambda t} \quad (39)$$

The copper sources irradiated had masses of 1 to 3 grams, and immediately after activation a significant radiation hazard existed. A 3 gram source irradiated in a flux of  $6.5 \times 10^{11}$   $\text{n cm}^{-2}\text{sec}^{-1}$  for 8 hours produced a radiation field of 10 rem/hr at one foot as measured by a "soft-shell" (ORNL chamber) cutie pie, an air ionization chamber. Thus the sources were manipulated with tongs behind a stack of 4-inch-thick lead bricks, and exposure time was kept at a minimum.

### C. Calibration

#### 1. Barium-137 Sources

A 21.4 mc barium-137 gamma source was used to determine an upper limit for the counting rate acceptable by the multichannel analyzer and to determine the efficiency of the NaI scintillation crystal.

The counting rate of a detector of area A exposed to a point source of monoenergetic radiation at a distance x is given by

$$I = \frac{\epsilon I_0 A}{4\pi x^2} \quad (40)$$

where  $\epsilon$  is the detector efficiency for radiation of that energy,  $I_0$  is the disintegration rate, and I is the detected count rate under the 662-keV photopeak. If  $Ix^2$  is plotted as a function of x, a straight line of zero slope should result. Such a plot is shown in Fig. 14. The falloff of  $Ix^2$  below  $x = 160''$  is due to the excessive count rate. At  $x = 140''$  the total pulse rate appearing at the analyzer input was 4000 counts per sec. It was concluded that a higher pulse rate would cause significant spectral distortion.

One may solve Equation (40) for the crystal efficiency and use the value  $Ix^2 = 9.7 \times 10^8$  in<sup>2</sup>/min from Fig. 14 to obtain

$$\epsilon = \frac{Ix^2 4\pi}{I_0 A} = 17.4\% \quad (41)$$

A small barium-137 gamma source was then calibrated by determining  $Ix^2$  and using the crystal efficiency of 17.4% in the equation

$$I_0 = \frac{4\pi Ix^2}{\epsilon A} \quad (42)$$

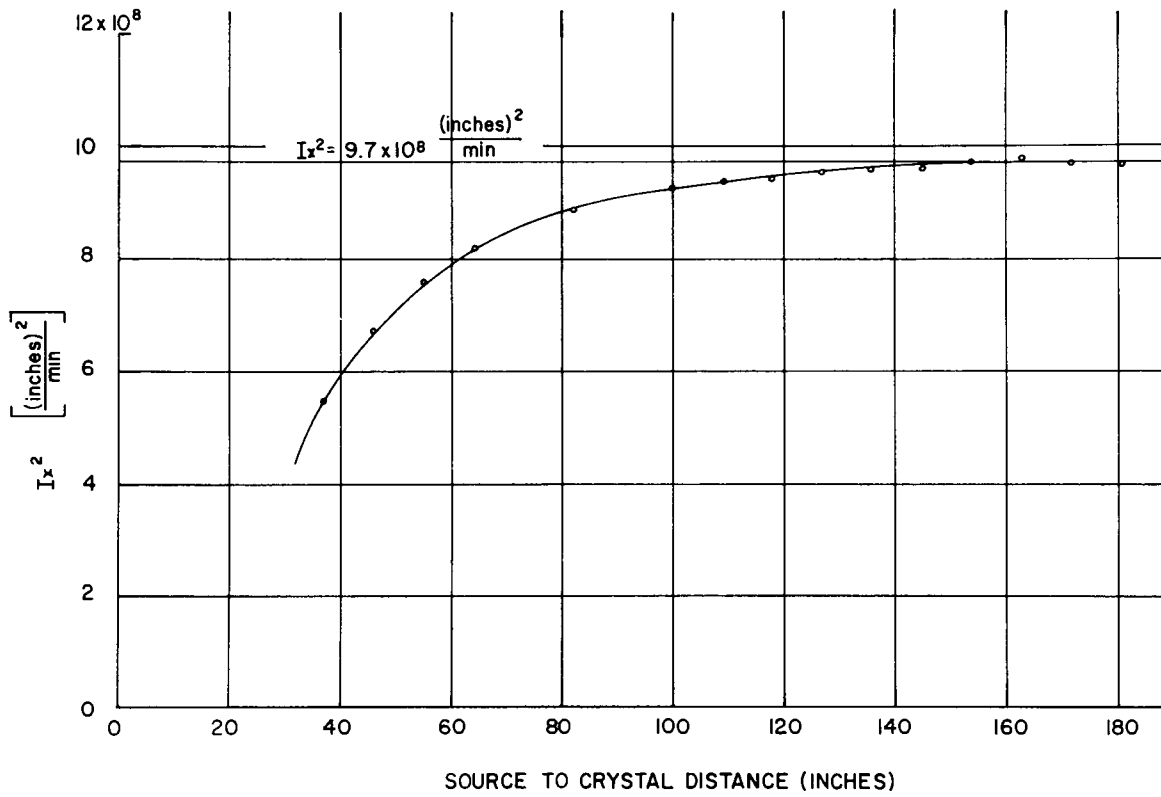
UNCLASSIFIED  
ORNL-LR-DWG. 70503

Fig. 14. Dependence of Efficiency of NaI(Tl) Scintillation.

The  $I_0$  value for this source was 3.0  $\mu\text{c}$ .

The anthracene crystal in the spectrometer was replaced by the 3  $\mu\text{c}$  barium-137 gamma source, and the ratio of the number of counts detected under the 662-keV photopeak in the NaI crystal to the number of gamma rays born in the source was determined. This value was found to be  $7.12 \times 10^{-4}$ . Considering only two-quanta annihilation processes, one may conclude that for every positron annihilating in the anthracene  $1.42 \times 10^{-3}$  pulses will appear at the output of the coincidence circuitry.

The bare barium-137 source was used to study the resolution of the spectrometer and to obtain an energy calibration for the analyzer.  $\text{Cs}^{137}$  decays<sup>46</sup> by beta emission to  $\text{Ba}^{137}$ , 92% of which is in an excited state. This state decays with a 2.6 minute half life to the ground state by gamma emission with an energy release of 661.6 keV (see Fig. 13). The internal conversion coefficient for the K-shell is 0.092, and the K-shell binding energy is 37.4 keV<sup>47</sup>. The internal conversion electron then has an energy of 624 keV which is significantly above the 514-keV maximum energy of the beta continuum.

Various anthracene crystals and geometries were tried with resolutions ranging from 9% to 14% as determined by the energy width

---

<sup>46</sup>RADIOLOGICAL HEALTH HANDBOOK, Division of Radiological Health, U. S. Department of Health, Education and Welfare, Washington, D. C. p. 333, (1960).

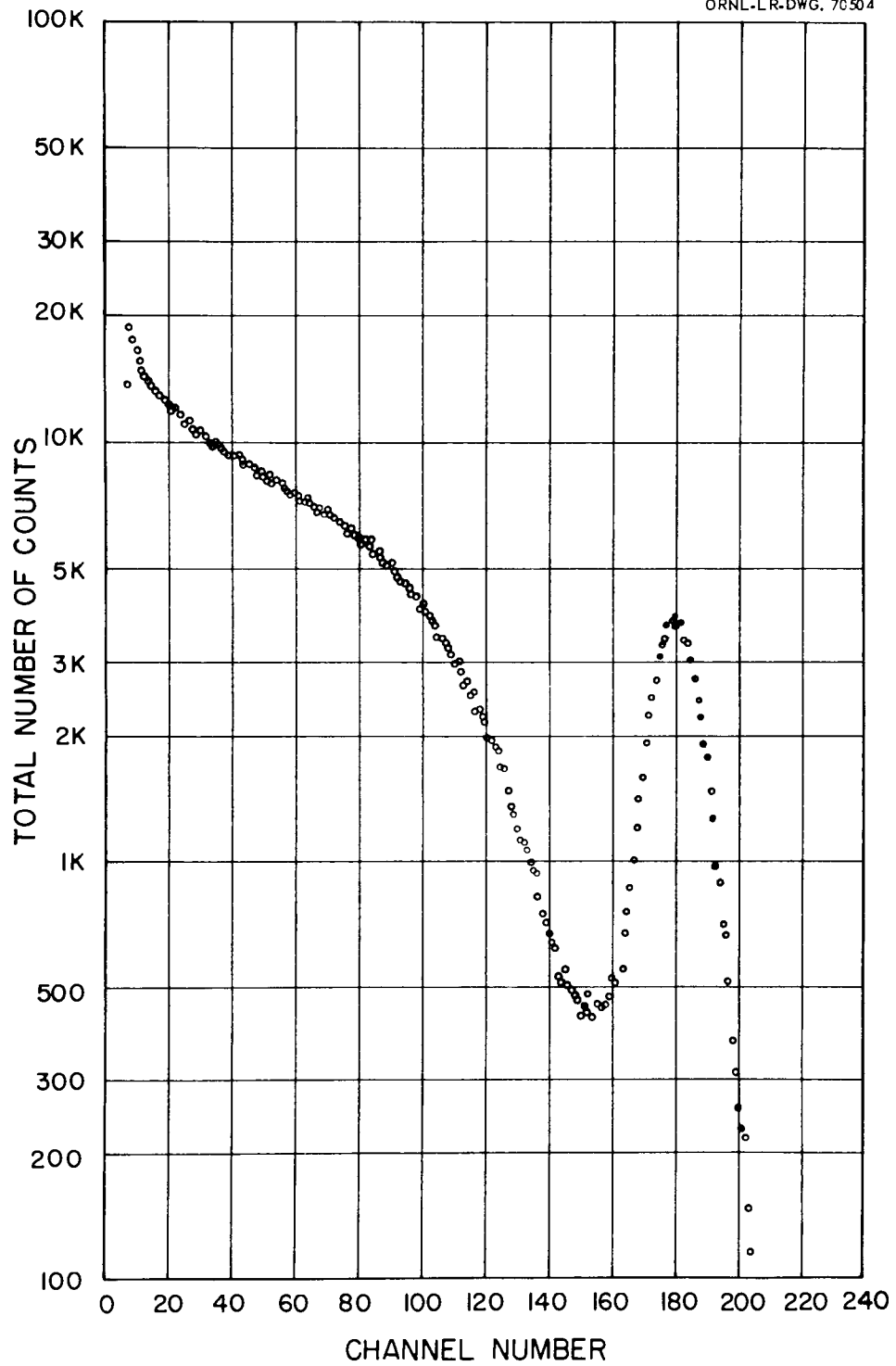
<sup>47</sup>HANDBOOK OF CHEMISTRY AND PHYSICS, eds. C. D. Hodgman, R. C. West and S. M. Selby, 38th ed., (Chemical Rubber Publishing Co. Cleveland, 1956) p. 296, 2437.

at half the peak height divided by 624. Fig. 15 shows a typical (Cs-Ba)<sup>137</sup> spectrum with an anthracene crystal 0.5 inch diameter x 0.08 inches thick.

## 2. Mercury Relay Pulse Generator

The pulse generator was particularly suitable for analyzer linearity studies and energy calibration because of its stability. In a temperature controlled laboratory from a regulated power line, the drift does not exceed 1/4 small dial division of the 10 turn helipot. The analyzer response curve as shown in Fig. 16 indicates slightly nonlinear behavior in the middle section. This nonlinearity was considered insignificant and was therefore ignored in the spectral analyses.

The energy calibration of the analyzer was accomplished in the following way. The voltage from the pulse generator was adjusted so that its amplified pulse fell in the channel corresponding to the <sup>624</sup> Ba<sup>137</sup> internal conversion electron peak. By keeping the same generator output or a known multiple of it and varying the gain of the appropriate channel of the dual amplifier, the analyzer could be calibrated to any desired energy range. For example, a calibration of 1 keV per channel would require that the amplifier be adjusted so that the generator pulse corresponding to the 624 keV peak would fall in a hypothetical channel 624 or a pulse of 1/3 this voltage would fall in channel 208.

UNCLASSIFIED  
ORNL-LR-DWG. 7C504Fig. 15.  $(\text{Cs-Ba})^{137}$  Beta Spectrum Using Anthracene Crystal.

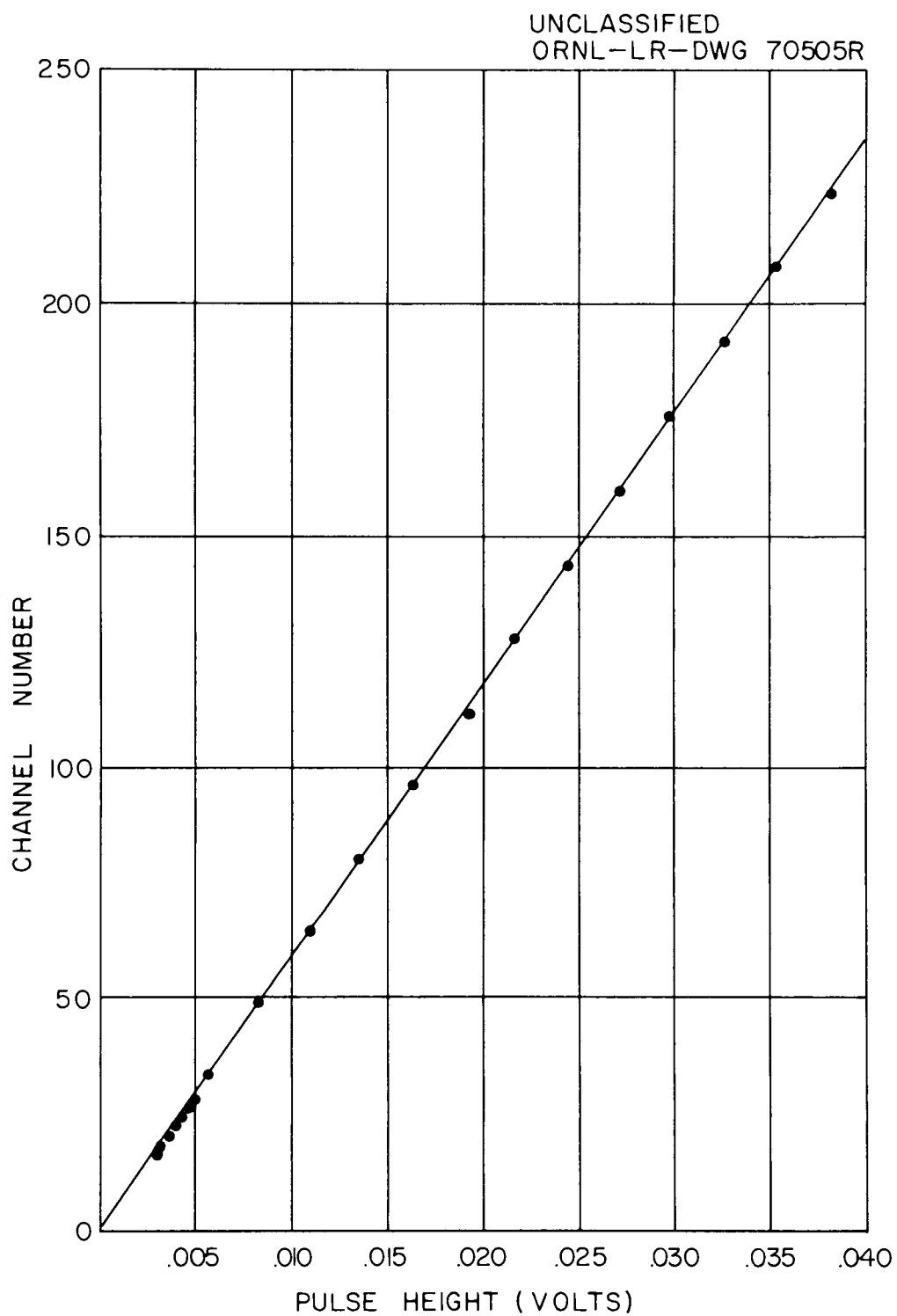


Fig. 16. Channel Number Versus Pulse Height For Pulse Height Analyzer.

## 3. Promethium 147 Spectrum and Corrections

Langer, et al.<sup>48</sup> studied the beta spectrum of  $\text{Pm}^{147}$  and found that it gave a linear Fermi plot above 8 keV with a 223-keV endpoint energy. Promethium 147 was used to examine the transmission of the anthracene spectrometer for these reasons, and because the method of decay is relatively simple (see Fig. 13). One obtains the Fermi plot of a beta spectrum by plotting  $\frac{N(p)}{f(Z,p)}$  as a function of energy where  $f(Z,p)$  is the Fermi function and  $N(p)$  is the experimental momentum distribution. The Fermi function is tabulated in the N.B.S. publication "Tables for the Analysis of Beta Spectra".<sup>49</sup> One may convert the energy spectrum found in this research into the momentum spectrum by using Equation (43).

$$N_1(p) = N(E) \frac{dE}{dp} \quad (43)$$

One may obtain  $\frac{dE}{dp}$  for relativistic electrons as follows: The relationship between kinetic energy  $E$  and momentum  $p$  is

$$E = \sqrt{p^2 c^2 + m_0^2 c^4} - m_0 c^2 \quad (44)$$

then

$$\frac{dE}{dp} = \frac{pc^2}{\sqrt{p^2 c^2 + m_0^2 c^4}} = \frac{m_0 v c^2}{\sqrt{1 - \beta^2}} \cdot \frac{\sqrt{1 - \beta^2}}{m_0 c^2} = v \quad (45)$$

<sup>48</sup>L. M. Langer, J. W. Motz, and H. C. Price, Jr., Phys. Rev. 77, 789-805 (1950).

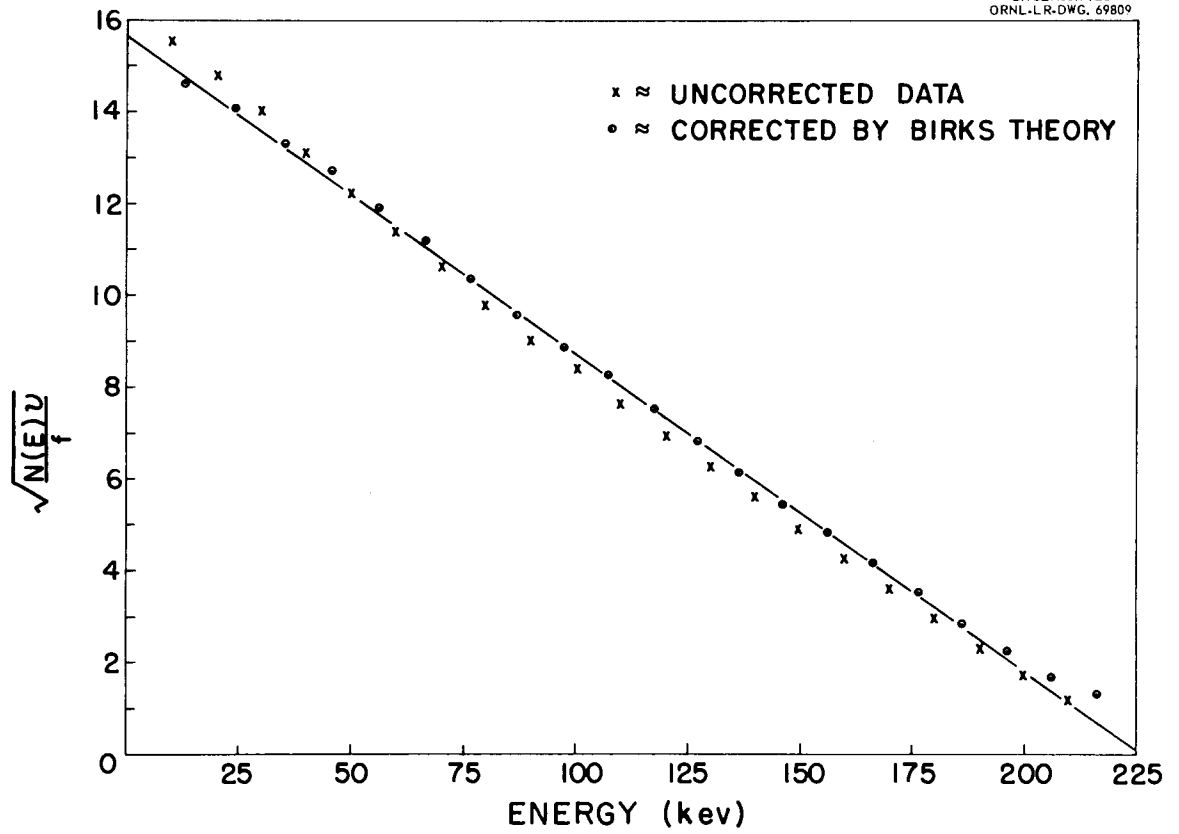
<sup>49</sup>National Bureau of Standards Applied Mathematics Series 13, "Tables for the Analysis of Beta Spectra," Washington, D. C. 46, (1932).

That is, to obtain the momentum distribution from the energy distribution  $N(E)$  one simply multiplies  $N(E)$  by  $v(E)$ .

Fig. 17 shows the Fermi plot obtained from the uncorrected spectrum compared with the Fermi plot one obtains after applying Birks' theory described in Section II-B. If one makes no correction for analyzer nonlinearity but considers only crystal nonlinearity, the number of counts recorded in a particular channel,  $C$ , is to be associated not with energy  $E = C \times K$  where  $K$  is the (Cs-Ba)<sup>137</sup> calibration in keV per channel but with an energy  $E'$  which is higher than  $E$  by the horizontal energy difference between the point on the linear response line in Fig. 2 corresponding to  $E$  and the actual response line corresponding to  $E'$ . The corrected Fermi plot appears linear except at energies near the endpoint where the resolution effect becomes apparent. The data were corrected for changes in bandwidth, but were not corrected for the statistical shift of the photomultiplier response at low energies due to the small average number of photoelectrons ejected at the photocathode,<sup>50</sup> scattering electrons from the collimators and source backing, or backscattering from the crystal surface. These phenomena have compensating effects, and the linearity at low energies is fortuitous and indicates a constant transmission spectrometer.

---

<sup>50</sup>G. T. Wright, Journal of Scientific Instruments 31, 462-465 (1954).

UNCLASSIFIED  
ORNL-LR-DWG. 69809Fig. 17. Fermi Plot of  $Pm^{147}$ .

## V. COPPER 64 SPECTRA

The Cu<sup>64</sup> positron spectrum was measured by coincidence scintillation techniques. A positron originating in the source struck and was absorbed in an anthracene crystal, thus producing a light pulse. The positron annihilated, and one 0.511 MeV gamma was detected by the NaI(Tl) crystal. A typical gamma spectrum of the annihilation radiation detected by the NaI(Tl) spectrometer is shown in Fig. 18. The photopeak for the 0.511-Mev gamma ray occurs around channel 119 in the spectrum. The amplifier associated with the NaI(Tl) crystal generated a gating pulse whenever a photoelectric interaction with the 0.511 MeV gamma was detected. This pulse was applied to the linear gate of the analyzer permitting the pulse from the anthracene photomultiplier to enter the analog-to-digital conversion (ADC) circuitry of the analyzer which then recorded the pulse in one of 256 channels. The spectral distribution recorded in this manner was compared with the flux predicted by the continuous-slowing-down model by means of the relation:

$$\bar{\phi}(E) = N(E) \frac{1}{G_1} \frac{1}{\epsilon} \frac{1}{G_2} \frac{1}{\bar{A}} \quad (46)$$

where  $\bar{\phi}(E)$  is the flux in units of positrons  $\text{cm}^{-2} \text{keV}^{-1} \text{sec}^{-1}$  predicted by the continuous slowing down model normalized to one positron born per  $\text{cm}^3$  per sec;  $N(E)$  is the average number of positrons detected per keV per sec during the counting period;  $G_1$  is the NaI(Tl) crystal geometry factor;  $\epsilon$  is the NaI(Tl) crystal photoelectric efficiency for 0.511 MeV gamma radiation;  $G_2$  is the anthracene geometry factor; and  $\bar{A}$  is the average number of positrons born per sec per  $\text{cm}^3$  during

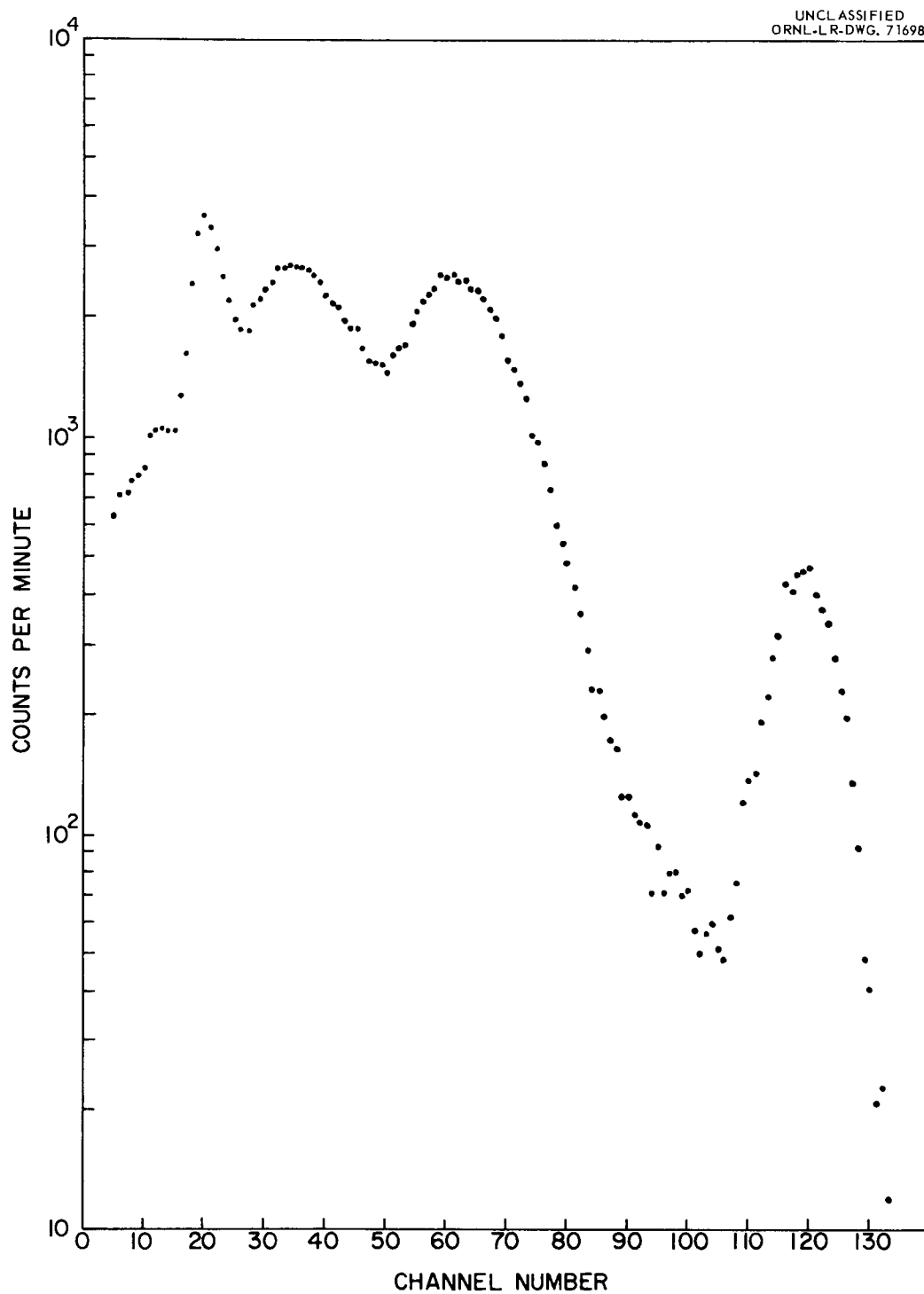


Fig. 18. Pulse Height Distribution for Annihilation Radiation in NaI(Tl).

the counting period. The geometry factor  $G_1$  was about  $8 \times 10^{-3}$  and  $\epsilon$  was about 0.17. The product  $G_1 \times \epsilon$ , however, was more precisely determined to be  $1.42 \times 10^{-3}$  (Section IV-C-1).  $G_2$  was  $1.7 \times 10^{-3}$  for an exposed crystal area of 1/2 inch and a source-to-crystal distance of 12 inches. For a positron spectrum obtained during time  $t_1$  to  $t_2$  from a source removed from the reactor at  $t_0$  with initial activity at removal of  $A_0$ , the factor  $\bar{A}$  is the average specific activity during the interval  $t_1$  to  $t_2$  and occurs at time  $t'$  given by:

$$t' = t_1 + \frac{1}{\lambda} \ln \left[ \frac{\lambda(t_2 - t_1)}{1 - e^{-\lambda(t_2 - t_1)}} \right] \quad (47)$$

as derived in the Appendix. One may calculate  $\bar{A}$  from Equation (52) in the Appendix:

$$\bar{A} = \frac{A_0 e^{-\lambda t_1}}{\lambda(t_2 - t_1)} \left[ 1 - e^{-\lambda(t_2 - t_1)} \right] \quad (48)$$

The experimental spectrum was corrected for anthracene nonlinearity by Birks' theory (Equation 23) and for the changing energy bandwidth (Equation 28) below 140 keV. The spectrum was also corrected for the correlated coincidence effect due to the interaction of the positron annihilation gamma as it escaped the crystal (see Section II-A-2). Chance coincidences for any type of radiation with a positron energy pulse gated by its annihilation gamma ray were possible only during the  $2\mu$  sec the linear gate was open for each positron pulse detected. The shift correction for this effect discussed in Section II-A-2 was less than 1 keV for the positron spectra measured.

Fig. 19 shows the positron spectrum of a plane source compared

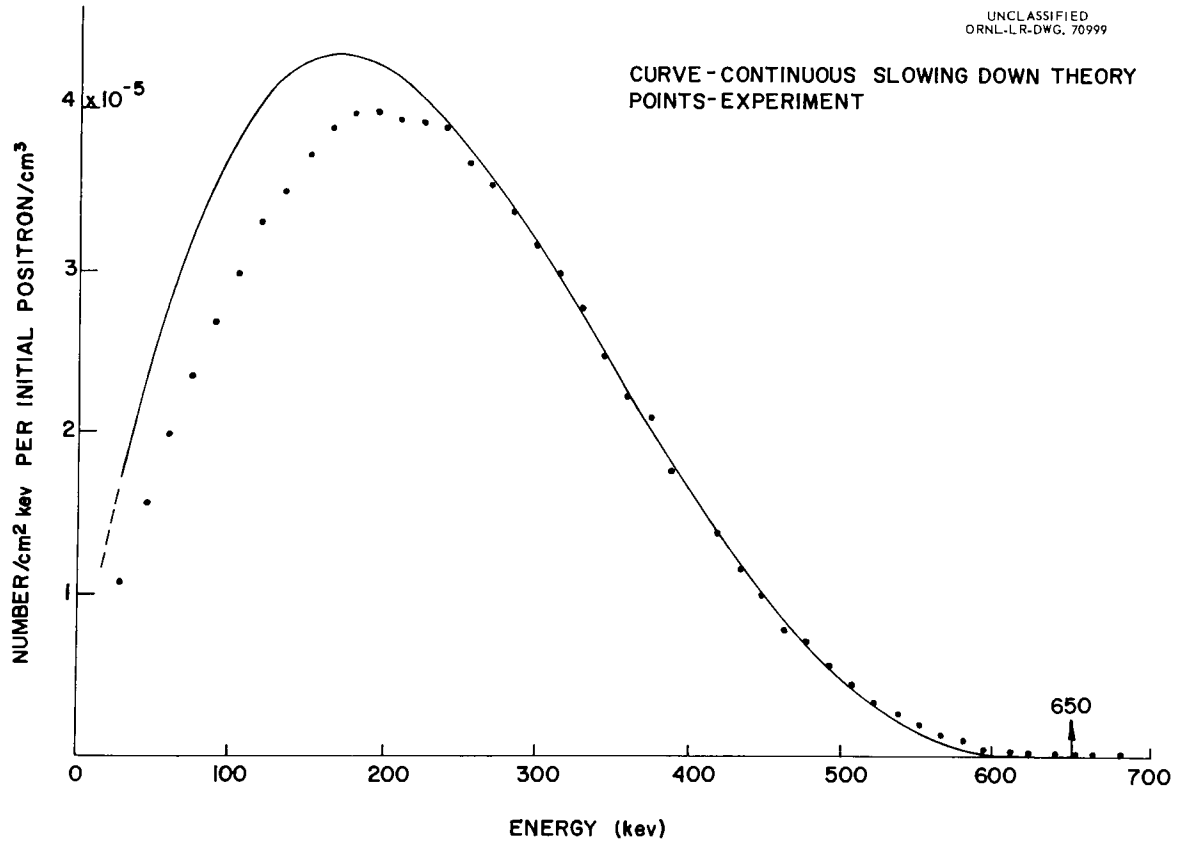


Fig. 19. Positron Spectrum from Plane Source of Cu<sup>64</sup> in Copper.

with the continuous-slowing-down theory. The positron spectrum was normalized with the continuous-slowing-down theory at 300 keV in order to show the expected deficiency of low energy positrons; i e. the absence of emitting walls adjacent to the plane source resulted in a loss of positrons originating in the walls and backscattering into the detector from the plane source. This backscattered contribution to the flux from the plane source has a degraded energy spectrum.

Fig. 20 shows the total anthracene crystal response to  $\beta$  and  $\gamma$  radiation from the plane source compared with the  $\gamma$  response only. The source was covered with a  $1/8$  inch thick lucite disc to obtain the  $\gamma$  response spectrum. Fig. 21 shows the same curves for the cavity sources with the expected lower  $\beta$  to  $\gamma$  ratio due to the smaller fractional surface area which could contribute to the beta flux. The positron slowing-down spectrum was separated from the total response spectrum by the coincidence technique described at the beginning of this section. Fig. 22 shows the experimental positron spectrum compared with the theory of the continuous-slowing-down model from Equation 5. The data were multiplied by a normalization factor of 1.6 in order to bring the data into agreement with the theory at 300 keV. No significance was given to this factor as it seemed to vary from source to source over the range of 0.75 to about 2.0.

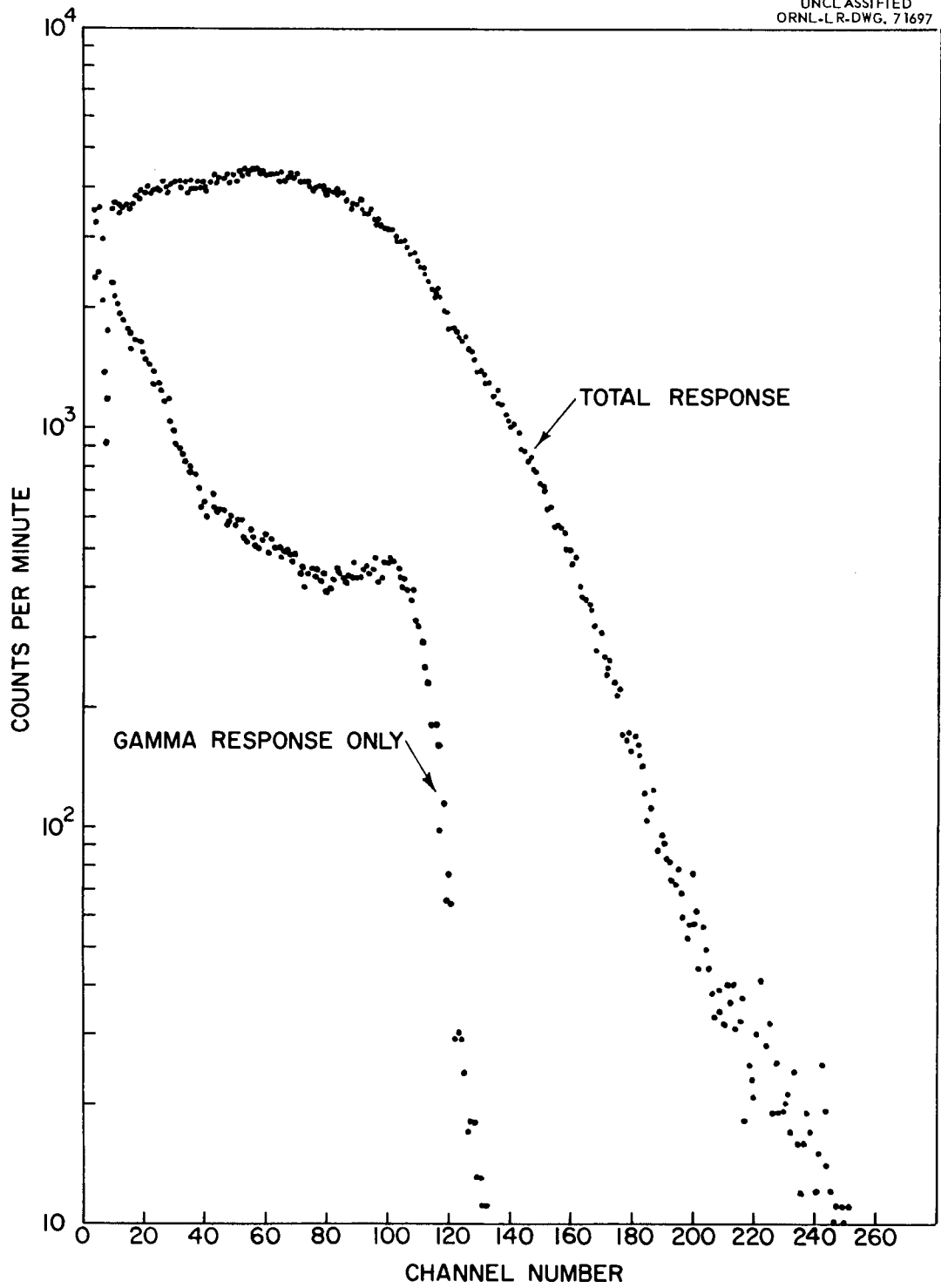


Fig. 20. Beta-Gamma Spectrum and Gamma Spectrum from a Plane Source  $\text{Cu}^{64}$ .

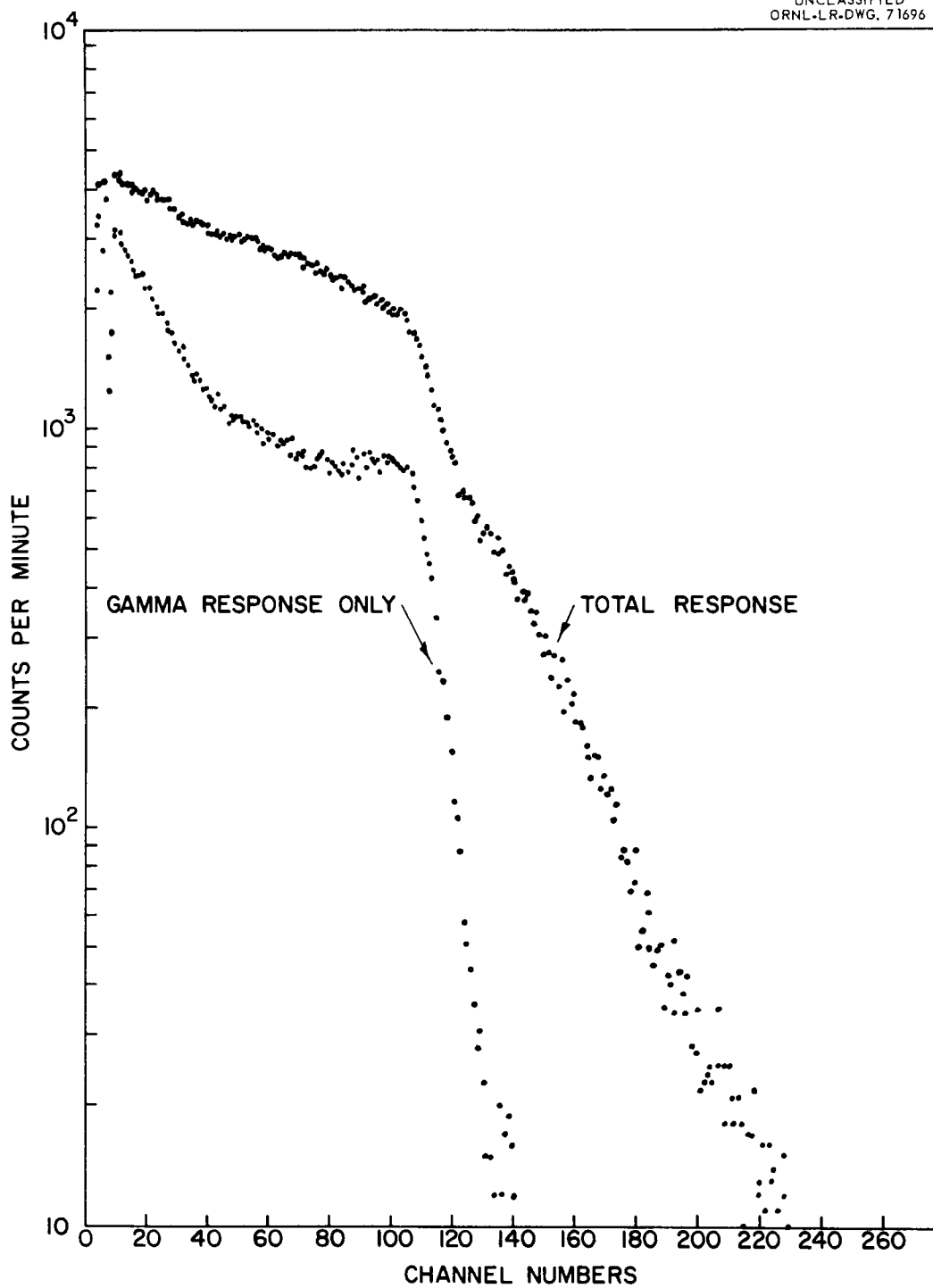


Fig. 21. Beta Gamma Spectrum and Gamma Spectrum from A Cavity Source of  $\text{Cu}^{64}$ .

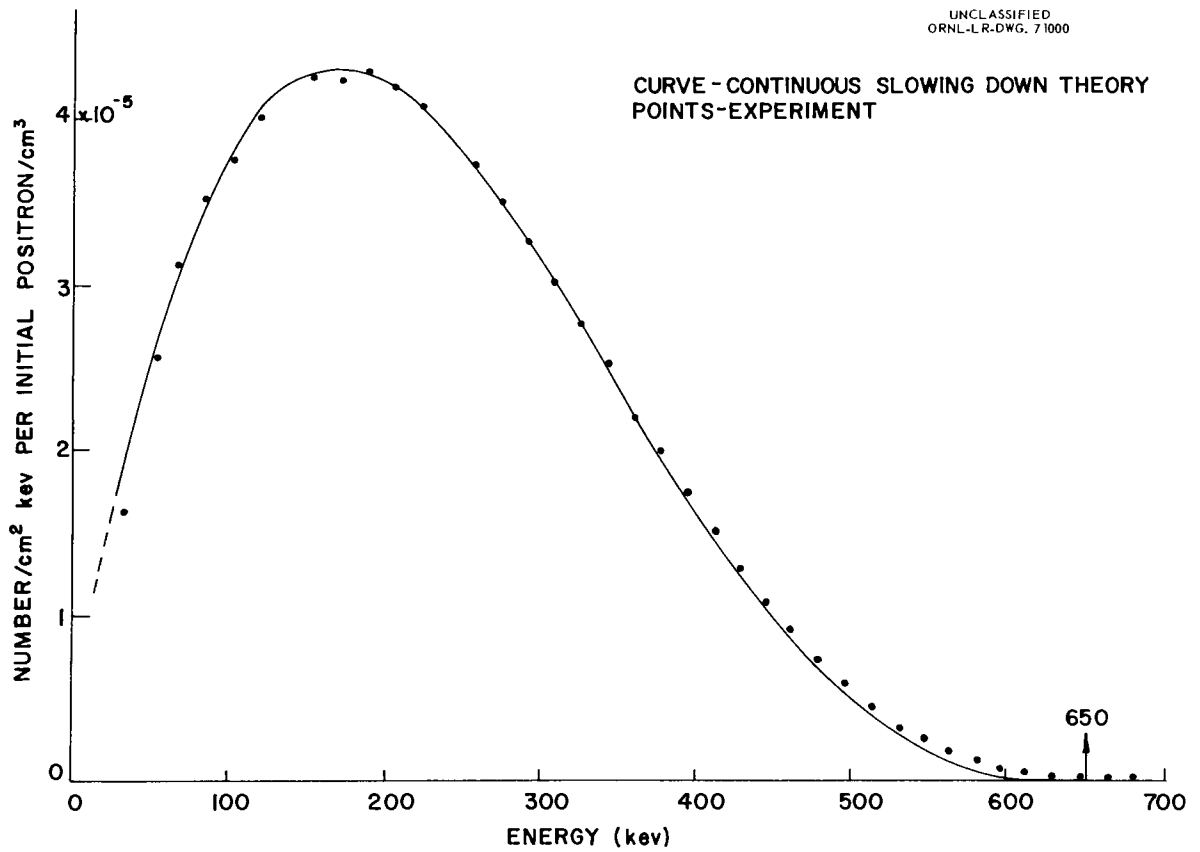


Fig. 22. Experimental Positron Flux and the Continuous-Slowing-Down Theory.

## VI. DISCUSSION

It may be concluded that a plane anthracene crystal-photomultiplier combination is suitable for beta spectroscopy, and that the spectral corrections described adequately correct the experimental data for the effects of anthracene nonlinearity, for changing energy bandwidth, and for the coincidence interaction of the positron annihilation gamma as it escapes the crystal.

The shape of the positron slowing-down spectrum in copper is correctly predicted by use of the continuous-slowing-down model, and the absolute magnitude of the positron flux inside the copper is within a factor of two of that predicted by the continuous-slowing-down model.

The spectrum of the positrons escaping the surface of a plane source thicker than the positron range is not identical with the slowing-down spectrum in an infinite medium due to a deficiency in the number of positrons with low energies.

## APPENDIX

## Determination of the Average Activity During a Time Interval

The activity of a source at any time  $t$  relative to the activity  $A_0$  at time  $t = 0$  is:

$$A = A_0 e^{-\lambda t} \quad (49)$$

The average activity during an interval  $t_1$  to  $t_2$  is given by:

$$\bar{A} = \frac{N_{12}}{(t_2 - t_1)} \quad (50)$$

where  $N_{12}$  is the total number of counts observed during the interval.

The average activity is equal to the actual activity at some time  $t'$ .

Since:

$$\begin{aligned} N_{12} &= \int_{t_1}^{t_2} A_0 e^{-\lambda t} dt \\ &= \frac{A_0 e^{-\lambda t}}{\lambda} \left[ 1 - e^{-\lambda(t_2 - t_1)} \right] \end{aligned} \quad (51)$$

then,

$$\bar{A} = A_0 e^{-\lambda t'} = \frac{A_0 e^{-\lambda t_1}}{\lambda(t_2 - t_1)} \left[ 1 - e^{-\lambda(t_2 - t_1)} \right] \quad (52)$$

Eq. (52) may be solved for  $t'$  with the result:

$$t' = t_1 + 1/\lambda \ln \left[ \frac{\lambda(t_2 - t_1)}{1 - e^{-\lambda(t_2 - t_1)}} \right] \quad (53)$$

## BIBLIOGRAPHY

- Bhattacharjee, S. K., Sahai, B., Baba, C.V.K., "Decay of  $Pm^{148}$ ,"  
Nuclear Phys. 12, 356-370 (1959).
- Birkhoff, R. D., Hubbell, H. H., Cheka, Jr., J. S., and Ritchie, R. H.,  
"Spectral Distribution of Electron Flux in a Beta-Radioactive  
Medium," Health Phys. 1, 27-33 (1958).
- Birks, J. B., and Brooks, F. D., "Scintillation Response of  
Anthracene to 6-30 keV Photoelectrons," Proc. Phys. Soc. (London)  
69B, 721 (1956).
- Birks, J. B. SCINTILLATION COUNTERS, (McGraw-Hill Book Co., Inc.,  
New York, 1953).
- Birks, J. B. "Scintillations from Organic Crystals: Specific  
Flourescence and Relative REsponse to Different Radiations,"  
Proc. Phys. Soc. (London) A64, 874 (1951).
- Bisi, A., Germagnoli, E., and Zappa, L., "Solid Scintillators for  
Beta Ray Spectrometry," Nuovo cimento (10) 3, 1007-1016 (1956).
- Cottini, C., Fabri, G., Gatti, E., Germagnoli, E., "On Positron  
Lifetime in Anthracene," Nuova cimento (10) 14, 454-455, (1959).
- Dirac, P.A.M., "On the Annihilation of Electrons and Positrons,"  
Proc. Cambridge Phil. Soc. 26, 361-375 (1930).
- Evans, R. D., THE ATOMIC NUCLEUS, (McGraw-Hill Book Co., Inc. New  
York, 1955).
- Fowler, J. M. and Roose, C. E., "Response of Anthracene and Stilbene  
to Low Energy Protons and X-Rays," Phys. Rev. 98, 996 (1955).
- Glocker, R., "Die Abhangigkeit der Reichweite der Elektronen von  
ihre Energie," Z. Naturforsch 3a, 147 (1948).
- Gubernator, K., Heckmann, R. H., and Flammersfeld, A., "Die  
Szintillations--Lichtausbeute von Anthrazen fur Positronen and  
Elektronen kleiner Energie," Z. Physik 158, 268-273 (1960).
- Hodgman, C. D., Weast, R. C. and Selby, S. M. eds., HANDBOOK OF  
CHEMISTRY AND PHYSICS, 38th ed. (Chemical Rubber Publishing Co.,  
Cleveland, 1956), p. 296 and 2437.

- Hoffman, K. W., "Die Lichtausbeute von Anthracen für Elektronen von 20 bis 160 keV," Z. Physik 148, 303-307 (1957).
- Hopkins, J. I., "Electron Energy Studies with the Anthracene Scintillation Counter," Rev. Sci. Instr. 22, 29 (1951).
- Hughes, D. J. and Schwartz, R. B., NEUTRON CROSS SECTIONS, 2nd ed. (Brookhaven National Laboratory, Upton, 1958) p. 8.
- Johnston, L. W., Birkhoff, R. D., Cheka, J. S., Hubbell, H. H., Saunders, B. G., "Response of the Anthracene Scintillation Counter to Low Energy Electrons," ORNL-2298, 1959, Oak Ridge National Laboratory, Oak Ridge, Tennessee.
- Lane, R. O. and Zaffarano, D. J., "Transmission of 0-50 Kilovolt Electrons by Thin Films with Applications to Beta-Ray Spectroscopy," Iowa State College, 439, 1953.
- Langer, L. M., Motz, J. W., Price, Jr., H. C., "Low Energy Beta-Ray Spectra:  $\text{Pm}^{147}$ ,  $\text{S}^{35}$ ," Phys. Rev. 77, 789-805 (1950).
- Libby, W. E., "Measurement of Radioactive Tracers," Analytical Chemistry 19, 2 (1947).
- Madansky, Leon, and Rasetti, Franco, "An Attempt to Detect Thermal Energy Positrons," Phys. Rev. 79, 397 (1950).
- McMaster, W. H., "Polarization Phenomena for Positron Annihilation-in-Flight," Nuovo cimento (10) 17, 395-414 (1960).
- National Bureau of Standards Applied Mathematics Series 13, "Tables for the Analysis of Beta Spectra," Washington, D. C. 46 (1952).
- National Bureau of Standards Circular 577 "Energy Loss and Range of Electrons and Positrons," Washington, D. C., 17 (1956).
- National Bureau of Standards Circular 542, "Graphs of the Compton Energy Angle Relationships and the Klein-Nishina Formula from 10 keV to 500 MeV," Washington, D. C. 84 (1953).
- National Bureau of Standards Supplement to Circular 577, "Energy Loss and Range of Electrons and Positrons," Washington, D. C., 13 (1958).
- Newman, E., Smith, A. M., and Steigert, F. E., "Fluorescent Response of Scintillation Crystals to Heavy Ions," Phys. Rev. 122, 1520-1524, (1961).

- RADIOLOGICAL HEALTH HANDBOOK, Division of Radiological Health, U. S. Department of Health, Education, and Welfare, Washington, D. C. (1960), pp. 333, 3336.
- Ramler, W. J., Freedman, M. S., "The Scintillation Efficiency of Anthracene for Low Energy Electrons," Rev. Sci. Instr. 21, 784-786 (1950).
- Robinson, W. H., and Jentschke, W., "Response of Anthracene Scintillation Crystals to Monoenergetic Soft X-Rays," Phys. Rev. 95, 1413 (1954).
- Rohrlich, F. and Carlson, B. C., Phys. Rev. 93, 38, 1954.
- Schneider, D. O. and Cormack, D. V., "Monte Carlo Calculations of Electron Energy Loss," Rad. Res. 11, 418-429 (1959).
- Siegbahn, K., ed., BETA-AND GAMMA-RAY SPECTROSCOPY, Interscience Publishers Inc., New York, (1955).
- Sokolnikoff, I. S. ADVANCED CALCULUS, McGraw-Hill Book Co., Inc. New York, (1939).
- Seitz, F. and Turnall, d., eds. SOLID STATE PHYSICS, Academic Press New York, Vol. 10, (1960).
- Spencer, L. V. and Fano, U., "Energy Spectrum Resulting from Electron Slowing Down," Phys. Rev. 93, 1172-1181 (1954).
- Subba Rao, B. N., "Effect of Window Absorption and Source Backing on  $\beta$ -Spectra," Proceedings of the Indian Academy of Sciences A51, 28-33 (1960).
- Taylor, C. J., Jentschke, W. K., Remley, M. E. Elby, F. S., and Druger P. G., "Response of Some Scintillation Crystals to Charged Particles," Phys. Rev. 84, 1034-1043 (1951).
- von Schmeling, Hans-Henning Kausch-Blecken, "Die Lichtausbeute organischer Szintillatoren fur Elektronen vol 1 bis 12 keV," Z. Physik 160, 520-526 (1960).
- Wallace, P. R., "Positron Annihilation in Solids and Liquids", SOLID STATE PHYSICS, Vol. 10, F. Seitz and D. Turnbull, Eds. Academic Press, New York.
- Wright, G. T., "Scintillation Response of Phosphors at Low Particle Energies," Phys. Rev., 96, 569-570 (1954).
- Wright, G. T. "Scintillation Response of Anthracene Crystals to Short Range Electrons," Physical Review 100, 588-590, (1955).

ORNL-3469  
 UC-34 - Physics  
 TID-4500 (23rd ed.)

## INTERNAL DISTRIBUTION

- |                                     |                                  |
|-------------------------------------|----------------------------------|
| 1. Biology Library                  | 127. R. H. Lafferty, Jr.         |
| 2-4. Central Research Library       | 128. C. E. Larson                |
| 5. Reactor Division Library         | 129. D. L. Mason                 |
| 6-7. ORNL - Y-12 Technical Library  | 130. K. Z. Morgan                |
| Document Reference Section          | 131. D. R. Nelson                |
| 8-57. Laboratory Records Department | 132. R. L. Shipp                 |
| 58. Laboratory Records, ORNL R.C.   | 133. M. J. Skinner               |
| 59. E. T. Arakawa                   | 134. J. A. Swartout              |
| 60. J. A. Auxier                    | 135. J. W. Wachter               |
| 61-110. R. D. Birkhoff              | 136. A. M. Weinberg              |
| 111. L. C. Emerson                  | 137-171. W. H. Wilkie            |
| 112. J. F. Emery                    | 172. J. C. Frye (consultant)     |
| 113. B. R. Fish                     | 173. G. M. Fair (consultant)     |
| 114. F. F. Haywood                  | 174. J. H. Hursh (consultant)    |
| 115. H. H. Hubbell                  | 175. R. L. Platzman (consultant) |
| 116-125. G. S. Hurst                | 176. E. P. Odum (consultant)     |
| 126. W. H. Jordan                   | 177. H. O. Wyckoff (consultant)  |

## EXTERNAL DISTRIBUTION

178. Lewis V. Spencer, Physics Department, Ottawa University, Ottawa, Kansas
179. Martin J. Berger, National Bureau of Standards, Washington, D.C.
180. John Laughlin, Memorial Sloan-Kettering Cancer Center, 410 East 68th Street, Department of Physics, New York, New York
181. Werner Brandt, Department of Physics, New York University, New York, New York
182. P. R. J. Burch, Department of Medical Physics, University of Leeds, The General Infirmary, Leeds, England
183. J. B. Birks, University of Manchester, Manchester, England
184. Lloyd W. Johnston, 5997 Hickam Drive, Dayton 3, Ohio
185. John I. Hopkins, Box 327, Davidson College, Davidson, North Carolina
186. L. G. Augenstein, Biology Research Center, Michigan State University, East Lansing, Michigan
187. L. S. Taylor, National Bureau of Standards, Washington, D.C.
188. P. L. Ziemer, Bionucleonics Department, Purdue University, West Lafayette, Indiana
189. V. B. Bhanot, Physics Department, Panjab University, Chandigarh-3, India
190. University of Chile, Box 2777, Institute of Science, Santiago, Chile
191. Research and Development Division, AEC, ORO
- 192-756. Given distribution as shown in TID-4500 (23rd ed.) under Physics category